JOURNAL OF GEOPHYSICAL RESEARCH, VOL. 104, NO. B3, PAGES 5097–5114, MARCH 10, 1999

Age constraints on crustal recycling to the mantle beneath the southern Chile Ridge: He-Pb-Sr-Nd isotope systematics

Marnie E. Sturm and Emily M. Klein
Division of Earth and Ocean Sciences, Nicholas School of the Environment
Duke University, Durham, North Carolina

David W. Graham
College of Oceanic and Atmospheric Sciences, Oregon State University, Corvallis

Jill Karsten
School of Ocean and Earth Science and Technology, University of Hawaii at Manoa

Abstract. Basalts from the four southernmost segments of the subducting Chile Ridge (numbered 1-4 stepping away from the trench) display large variations in Sr, Nd, Pb, and He isotope and trace element compositions. *Klein and Karsten* [1995] showed that segments 1 and 3 display clear trace element evidence for recycled material in their source (e.g., low Ce/Pb). The uniformly mid-ocean ridge basalt (MORB)-like $^{3}He/^{4}He$ and modest variations in Pb, Sr, and Nd isotopes of segment 1 (nearest the trench) suggest recent (<20 Ma) introduction of a contaminant into its source, consistent with recycling of material from the adjacent subduction zone. In contrast, segment 3 lavas display a dramatic southward increase in enrichment, extending to highly radiogenic Pb and Sr isotopic compositions (e.g., $^{206}Pb/^{204}Pb = 19.5$) and the lowest $^{3}He/^{4}He$ yet measured in MORB ($3.5R_A$). The segment 3 variations are most readily explained by ancient (~2 Ga) recycling of terrigenous sediment and altered crust, but we cannot rule out more recent recycling of material derived from a distant continental source. The similarity in isotopic signatures of segment 4 lavas to Indian Ocean MORB extends the Dupal anomaly to the Chile Ridge. Like Indian Ocean MORB, the segment 4 isotopic variations are consistent with contamination by anciently recycled pelagic sediment and altered crust and require a complex history involving at least three stages of evolution and possibly a more recent enrichment event. Southern Chile Ridge MORB reflect the extensive degree of heterogeneity that is introduced into the depleted upper mantle by diverse processes associated with recycling. These heterogeneities occur on a scale of ~50-100 km, corresponding to transform- and propagating-rift-bounded segmentation, and attest to the presence of distinct chemical domains in the mantle often bounded by surficial tectonic features that maintain their integrity on the scale sampled by melting.

1. Introduction

It has been recognized for more than three decades that the suboceanic mantle is chemically and isotopically heterogeneous on a range of scales. Various origins for distinct types of heterogeneities in the upper mantle have been proposed, such as entrainment and dispersal of plume or "primitive" mantle material or recycling of crustal or lithospheric material at subduction zones [e.g., *Armstrong*, 1968; *Schilling et al.*, 1985; *Allègre et al.*, 1984; *Allègre and Turcotte*, 1985; *Hofmann and White*, 1982; *Ringwood*, 1982; *Zindler et al.*, 1982; *McKenzie and O'Nions*, 1983; *Rehkämper and Hofmann*, 1997]. Studies of processes occurring at subduction zones show that while some of the subducting lithosphere is immediately partitioned to the continent in arc magmas or by accretion, a substantial portion is returned to the mantle and may ultimately become entrained in the upper or lower mantle [e.g., *Hofmann and White*, 1980, 1982; *Chase*, 1981; *White*, 1985; *le Roex et al.*, 1989; *Plank and Langmuir*, 1998]. Indeed, lava compositions from some hot spots, such as the Azores, the Society Islands, and Gough Island, show strong evidence of recycled material in their source [e.g., *White and Hofmann*, 1982; *Weaver*, 1991a, b; *Chauvel et al.*, 1992; *Devey et al.*, 1990; *Dupuy et al.*, 1987].

It has been noted that some mid-ocean ridge basalts (MORB), far removed from hotspot influences, also display geochemical characteristics of recycled materials in their source [e.g., *Mahoney et al.*, 1992]. *Rehkämper and Hofmann* [1997], for example, suggested that the distinctive trace element and isotopic signatures of some Indian Ocean MORB result from large-scale mixing of anciently subducted oceanic crust and a small amount of pelagic sediment into the depleted upper mantle. Furthermore, *Niu and Batiza* [1997] argued that the trace element signatures of eastern Pacific seamounts result from mixing of subducted oceanic crust into the depleted upper mantle with subsequent upwelling, melting, and dispersal of the enriched material as mobile metasomatic fluids. The com-

Paper number 1998JB900107.
0148-0227/99/1998JB900107$09.00

mon theme in these and other studies is that the observed chemical enrichments originate through ancient recycling, and therefore the age and location of these recycling events remain obscure.

In a recent study of MORB from the southern Chile Ridge, *Klein and Karsten* [1995] reported trace element evidence for contamination of the mantle by recycled sediment and altered oceanic crust (Figures 1 and 2). The southern Chile Ridge provides an interesting location to study recycling because it is one of the few modern examples of spreading center subduction (Figure 1) [*Cande and Leslie*, 1986]. Previous geophysical and theoretical work on the subduction of spreading centers suggests that the downgoing lithosphere may develop a slab window [*Dickinson and Snyder*, 1979; *Thorkelson*, 1996] or may break up in the subduction zone [*van den Buekel*, 1990] thus providing a potential pathway or mechanism for contaminating the adjacent suboceanic mantle with slab-derived material. Drawing upon these ideas, *Klein and Karsten* [1995] raised the possibility that the trace element signature of recycling among some of the Chile Ridge lavas may have been introduced into the subridge mantle recently at the adjacent subduction zone.

While trace element studies may provide evidence for crustal recycling of material to the MORB source and potentially distinguish one type of contaminant from another, they cannot constrain the age of the contaminant and therefore whether the recycled chemical signature of the Chile Ridge MORB is related to recent recycling from the adjacent subduction zone. Radiogenic isotope studies of these lavas, however, can provide constraints on both the timing of the contamination event and the origin of the recycled materials. In this study we combine constraints from He, Pb, Sr, and Nd isotope systematics with those of trace elements to explore whether the recycled signature in some Chile Ridge lavas may be related to a recent recycling event at the adjacent subduction zone.

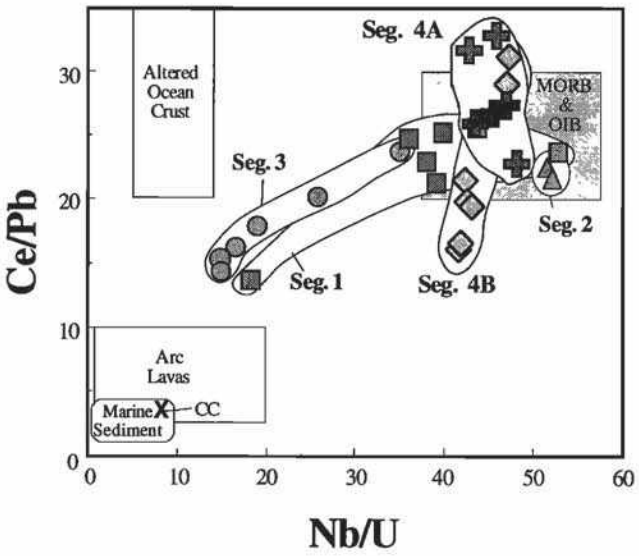

Figure 2. Nb/U versus Ce/Pb for Chile Ridge glasses after *Klein and Karsten* [1995] (symbols as in Figure 1). Also shown are fields for mid-ocean ridge basalts (MORB) and most ocean island basalts (OIB) [*Sun and McDonough*, 1989; *Hofmann et al.*, 1986, *Hofmann*, 1988; *Hickey et al.*, 1986], marine sediments [*Ben Othman et al.*, 1989; *Plank and Langmuir*, 1993; *Plank and Ludden*, 1992], arc lavas [*Hickey et al.*, 1986], altered oceanic crust (estimate modified from *Hart and Staudigel*, [1989] *Chauvel et al.*, [1992] *Plank*, [1993] *Staudigel et al.*, [1995]) and average upper continental crust (cross labeled CC; *Taylor and McLennan*, [1985]). Lavas from segments 1 and 3 extend from the MORB field toward compositions commonly associated with arc lavas, suggesting contamination of the mantle source with a small amount of sediment and altered crust [*Klein and Karsten*, 1995].

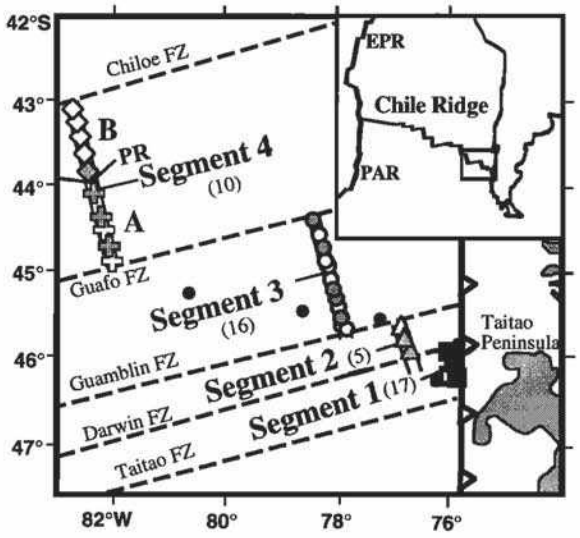

Figure 1. Tectonic elements of the southern Chile Ridge near its intersection with the Chile Trench. Ridge segments are labeled 1-4 with increasing distance from the trench (barbed vertical line). Fracture zones (FZ) are shown as dashed lines. Propagating rift (PR) is shown. Dredging and wax coring sites along each segment are as follows: segment 1 (squares), segment 2 (triangles), segment 3 (circles), segment 4A (crosses), segment 4B (diamonds), off-axis sites (small solid circles). Solid symbols along the ridge indicate samples analyzed for helium isotope composition. Inset shows regional location of the study area (box): East Pacific Rise (EPR); Pacific-Antarctic ridge (PAR).

2. Geologic Setting and Background

The Chile Ridge separates the Nazca and Antarctic plates and is currently being subducted beneath the South American plate near ~47°S at a rate of ~9 cm/yr [*Cande and Leslie*, 1986]. The southern Chile Ridge is an intermediate rate spreading center (~60 mm/yr full rate) that is generally characterized by a broad (10-20 km wide), deep (3400-4300 m) rift valley [*Klein and Karsten*, 1995; *Cande and Leslie*, 1986]. In January 1993 a dredging, wax coring, and mapping program was conducted along the four southernmost segments of the southern Chile Ridge, bounded by the Chile Margin Triple Junction in the south and the Chiloe Fracture Zone in the north, in order to investigate geochemical variations along the ridge axis as a function of distance from the trench (Figure 1). For convenience, these first-order ridge segments are numbered 1-4, with increasing distance from the trench. Detailed descriptions of the morphology of each segment are provided elsewhere [*Karsten et al.*, 1996; *Sherman et al.*, 1997]. Volcanic rock and glass fragments were recovered at 52 sites; all sites were located in the axial valley, with the exception of three sites which sampled two near-ridge seamounts (stations 24 and 55) and a short elevated off-axis ridge east of segment 1 (station 12).

Initial trace element results showed that a large number of lavas from the southern Chile Ridge are unlike the majority of MORB or most ocean island basalts (OIB) sampled previously [e.g., *Klein and Karsten*, 1995]. Specifically, samples from segments 1 and 3 extend well outside the MORB field toward low Nb/U, Ce/Pb, and Rb/Cs and high Th/La, compositions commonly associated with arc lavas (Figure 2). In addition, lavas from segment 4 extend toward low Ce/Pb and high Th/La but at MORB-like values of Nb/U (Figure 2). Major element systematics suggest that both normal MORB (NMORB) (K/Ti < 0.15) and enriched MORB (EMORB) (K/Ti > 0.15) collected along all four segments have experienced variable extents of low-pressure fractionation but have been generated by relatively uniform extents and pressures of melting [*Sherman et al.*, 1997]. The absence of systematics in melting parameters with distance from the trench suggests that mantle temperature and spreading rate (and not spreading ridge subduction) exert primary control on the southern Chile Ridge thermal regime [*Sherman et al.*, 1997].

3. Methods

Pb, Sr, and Nd isotope ratios were determined on 21 basalt glass samples (Table 1), hand-picked under a binocular microscope to avoid alteration and phenocrysts. To remove possible surface contamination, samples were mildly leached for 10 min. in weak HNO_3 and rinsed ultrasonically in deionized water. Sr and Nd analyses were performed on ~250 mg of sample following standard cation exchange techniques [*Hart and Brooks*, 1977; *Richard et al.*, 1976]. Pb isotope analyses were performed on a separate aliquot of ~250 mg of sample, using a chemical separation technique patterned after that of *Manhes et al.* [1978]. All Sr, Nd, and Pb isotope measurements were performed on a VG-SECTOR 54 mass spectrometer at the University of North Carolina at Chapel Hill. A few samples were spiked with a mixture of enriched ^{150}Nd, ^{149}Sm, ^{87}Rb, and ^{84}Sr for isotope dilution determinations of Nd, Sm, Rb, and Sr; these results agree well with inductively coupled plasma mass spectrometry (ICP-MS) determinations [*Klein and Karsten*, 1995; E. M. Klein et al., manuscript in preparation, 1998]. Blanks and standard measurements are reported in the Table 1 footnotes.

Helium isotope ratios were determined on a subset of 14 samples (Table 1; sample locations shown in Figure 1). Large glass chunks (~50 mg) were hand-picked under a binocular microscope and were ultrasonically cleaned with ethanol and deionized water. 150-250 mg of each sample were loaded into a stainless steel canister and crushed in vacuum using a solenoid-actuated piston made of magnetic stainless steel. Crushed powders of 10 samples remaining from these analyses were sieved to <100 μm and melted in a resistively heated furnace. All measurements were performed in the laboratory of J. Lupton at the National Oceanic and Atmospheric Administration (NOAA) Pacific Marine Laboratory in Newport, Oregon, on a double collector mass spectrometer designed for high-precision helium analyses as described by *Graham et al.* [1990]. Blanks were run before every analysis and were negligible (see Table 1).

4. Results

He, Pb, Sr, and Nd isotope compositions of southern Chile Ridge glasses are presented in Table 1 and Figures 3 and 4; also included in Table 1 for convenience are Rb, Sr, Sm, Nd, U, Th, and Pb abundances analyzed by ICP-MS and reported elsewhere [*Klein and Karsten*, 1995; E. M. Klein et al., manuscript in preparation, 1999] and He contents determined both by crushing and fusion of the remaining powders. As a whole, the Chile Ridge lavas are unusually diverse in isotopic composition, encompassing much of the variability among MORB worldwide. In addition, each ridge segment exhibits unique isotopic systematics.

4.1. Segment 1

Although segments 1 and 3 display similar trace element systematics (Figure 2), the two segments have markedly different isotopic characteristics. Despite their wide variability in trace element compositions extending from NMORB Ce/Pb (26) in the north to arc lava-like Ce/Pb (13) nearest the trench, segment 1 lavas have a restricted range in Sr ($^{87}Sr/^{87}Sr \approx 0.7027$), Nd ($^{143}Nd/^{144}Nd \approx 0.51310$), and Pb isotope composition (e.g., $^{206}Pb/^{204}Pb = 18.2$-18.4; Figure 3). Furthermore, they exhibit uniform and MORB-like $^3He/^4He$ (7.94-8.03 R_A; R_A is atmospheric ratio of $1.39X10^{-6}$; Figure 3b). Compared to MORB worldwide, segment 1 lavas generally lie in the region of overlap between Atlantic-Pacific MORB and Indian MORB, i.e., they have slightly elevated $^{208}Pb/^{204}Pb$ and $^{207}Pb/^{204}Pb$ for a given $^{206}Pb/^{204}Pb$ (Figure 4).

4.2. Segment 3

Segment 3 lavas form a dramatic north-to-south spatial gradient in isotope compositions (Figure 3). They range from NMORB compositions in the north (e.g., $^{206}Pb/^{204}Pb = 18.3$, ($^{87}Sr/^{87}Sr = 0.7025$, $^3He/^4He = 7.84\ R_A$, Ce/Pb=23.8) to highly radiogenic and enriched values in the south (e.g., $^{206}Pb/^{204}Pb = 19.5$, ($^{87}Sr/^{87}Sr = 0.70407$, Ce/Pb=13.5) and notably extend to the lowest $^3He/^4He$ yet measured in MORB (3.5 R_A). An off-axis seamount (D55-5) located near the southern end of segment 3 displays an isotopically extreme version of the segment 3 enrichment (Table 1). Compared to oceanic basalts sampled elsewhere, segment 3 lavas show some Pb-Sr-Nd isotopic affinities with lavas from the Society Islands [*Devey et al.*, 1990; *Chauvel et al.*, 1992; *Palacz and Saunders*, 1986; *Staudacher and Allègre*, 1989], although they extend to more radiogenic Pb isotope values and have unusually low $^{143}Nd/^{144}Nd$ for a given $^{87}Sr/^{87}Sr$ compared to Society lavas [Hart, 1986] (Figure 4a). The closest known hotspots to the study area, manifest in the islands of Juan Fernandez and San Felix located more than 1000 km north, possess Pb isotope compositions similar to the more radiogenic basalts of segment 3 but, in contrast, have high $^3He/^4He$ (up to 18 R_A [*Farley et al.*, 1993]), a signature which is absent along the southern Chile Ridge.

4.3. Segment 2

The limited sampling of segment 2 displays a north-to-south trend from modestly higher $^{87}Sr/^{87}Sr$ and $^{206}Pb/^{204}Pb$ (e.g., $^{87}Sr/^{87}Sr = 0.7030$) and lower $^{143}Nd/^{144}Nd$ and $^3He/^4He$ (e.g., $^3He/^4He = 6.4\ R_A$) in the north to values more typical of NMORB in the south (e.g., $^{87}Sr/^{87}Sr = 0.7025$, $^3He/^4He = 7.5\ R_A$). The relatively more enriched compositions in the north resemble the enriched chemical composition of southern segment 3 lavas (Figure 3) and may indicate some contamination of northern segment 2 subridge mantle with a source similar to that of southern segment 3. As a whole, the seg-

Table 1. Isotopic and Elemental Data for Chile Ridge Glasses and Local Surface Sediment

	Segment	Material	Lat., °S	Long., °W	Depth, m	$^{206}Pb/^{204}Pb$	$^{207}Pb/^{204}Pb$	$^{208}Pb/^{204}Pb$	$^{87}Sr/^{86}Sr$	$^{143}Nd/^{144}Nd$	$^{3}He/^{4}He$ (R/RA)	Sr	Pb	Th	U	Rb	Nd	Sm	[He] (μcm³ STP/g) Crushed	Melted
D10-5	1	glass	45°54.60'	75°57.06'	3218	18.268	15.527	37.968	0.702668	0.513119	7.94	117	0.619	0.341	0.091	2.89	13.01	4.48	6.41	
D14-9	1	glass	45°57.19'	75°56.06'	3248	18.165	15.519	37.912	0.702668	0.513149	8.03	123	0.332	0.132	0.033	1.02	8.02	2.81	6.53	5.76
D15-3	1	glass	45°57.19'	75°56.50'	3298	18.270	15.500	37.870	0.702671			124								
D20-1	1	glass	46°02.43'	75°53.80'	3304	18.398	15.553	38.179	0.702719	0.513113	7.98	133	0.767	0.497	0.131	4.45	9.33	3.06	5.46	2.11
D33-3	2	glass	45°42.55'	76°52.12'	4116	18.044	15.531	38.078	0.703002		6.39	66	0.305	0.236	0.043	2.62	6.90	2.54	2.78	
D34-1	2	glass	45°46.88'	76°46.79'	3993	17.930	15.490	37.689	0.702674	0.513162	7.46	88	0.315	0.117	0.023	1.11	8.57	3.15	0.42	
D35-2	2	glass	45°50.01'	76°45.75'	3730	17.843	15.490	37.501	0.702481	0.513205		231	0.436	0.078	0.023	0.32	8.36	2.64		
D41-1	3	glass	45°38.31'	77°50.76'	2874	19.103	15.642	39.099	0.704164	0.512669		292	1.266	1.223	0.341	13.65	14.32	3.86		
D42-4	3	glass	45°38.77'	77°53.35'	2909	19.489	15.688	39.556	0.704072	0.512709	3.51	255	1.313	1.441	0.379	12.34	12.56	3.35	0.48	3.30
D43-1	3	glass	45°30.35'	77°57.76'	2718	19.380	15.675	39.431	0.703750	0.512720	3.79	275	1.085	1.282	0.330	10.76	11.46	3.16	4.18	0.28
D47-1	3	glass	45°14.54'	78°06.48'	3236	19.282	15.662	39.286	0.703692		4.39	214	0.878	1.006	0.263	9.02	10.29	2.99	14.27	5.65
D51-1	3	glass	44°47.45'	78°16.56'	3563	18.787	15.580	38.632	0.703048	0.513043	6.60	107	0.522	0.415	0.108	3.43	9.02	3.01	0.21	0.43
D53-2	3	glass	44°32.33'	78°18.91'	3523	18.307	15.541	38.032	0.702487	0.513146	7.84	103	0.348	0.175	0.049	1.35	8.00	2.74	3.83	5.97
D58-4	4A	glass	44°57.10'	81°56.20'	3798	18.213	15.560	38.133	0.702519	0.513153		85	0.286	0.192	0.044	1.17	7.50	2.80		
D59-7	4A	glass	44°45.99'	82°00.48'	2703	18.401	15.649	38.446	0.703187	0.513007	7.62	184	0.301	0.555	0.132	4.12	7.42	2.52	2.38	1.18
D61-1	4A	glass	44°27.81'	82°10.82'	4060	18.133	15.496	37.713	0.702554	0.513188	8.41	99	0.322	0.166	0.061	1.31	10.26	3.67	7.98	0.71
D62-2	4A	glass	44°11.68'	82°14.09'	3900	18.029	15.487	37.639	0.702452	0.513218	8.35	85	0.274	0.084	0.020	0.44	6.93	2.59	0.38	7.21
D63-5	4B	glass	43°52.38'	82°25.64'	3853	17.953	15.524	38.314	0.703552	0.512900	7.97	150	1.054	1.132	0.245	11.36	8.71	2.35	10.17	
D65-1	4B	glass	43°26.24'	82°34.63'	3615	18.040	15.480	37.980	0.702966			139	0.639	0.619	0.150	6.00	9.34	2.83		
D66-2	4B	glass	43°06.63'	82°38.44'	3634	17.987	15.545	38.238	0.702996	0.513011		155	0.755	0.738	0.167	6.30	9.65	2.81		
D66-4	4B	glass	43°06.63'	82°38.44'	3634	18.040	15.460	37.590	0.702427			100	0.354	0.284	0.072	1.67	10.44	3.62		
d12-8		whole rock	45°55.19'	75°54.89'	2919	18.288	15.588	38.179	0.703914			150	9.356	8.134	2.185	71.65	18.20	4.24		
55-5	seamount	glass	45°25.90'	78°40.71'	1799	19.970	15.710	40.000	0.704548			308	2.257	3.590	1.211	12.34	25.28	6.12		
24-1	seamount	mud	46°07.83'	76°01.36	1980	18.674	15.595	38.581				240	14.780	3.840	1.640	24.43	18.01	4.25		

Chile Ridge glasses (segments 1-4) analyzed in this study and shown in Figure 1 are given. Also included are analyses of samples from a seamount just west of the southern portion of segment 3 (D55-5), a small off-axis ridge east of segment 1 (D12-8), and a surface mud sample from segment 1 (D24-1). Depth, determined by 3.5 or 12 kHz echo-sounding, is the average for dredge on bottom and off bottom. Isotope data are internally normalized to 0.11940 for $^{86}Sr/^{88}Sr$, and 0.72190 for $^{146}Nd/^{144}Nd$. Replicate standard analyses averaged 0.710243 for $^{87}Sr/^{86}Sr$ for NBS-987 and 0.511855 and 0.512136 for $^{143}Nd/^{144}Nd$ for the La Jolla and Ames standards, respectively. For one batch of Sr isotope analyses, higher NBS-987 values were obtained, requiring an interlaboratory bias correction of –0.01% (duplicate measurements from runs not requiring correction agree to within 0.005% of corrected values). Measured analytical uncertainties ($2\sigma/\sqrt{N}$) for Sr and Nd isotope ratios are generally < ±0.000023 and < ±0.000015, respectively. Pb data are referenced to the following values for NBS-981: 16.937, 15.491 and 36.721 for $^{206}Pb/^{204}Pb$, $^{207}Pb/^{204}Pb$, and $^{208}Pb/^{204}Pb$, respectively (replicate standard analyses yield a mean mass fractionation correction factor of 0.06%/amu). Duplicate Pb isotope measurements were made on separate dissolutions of two samples (averages are reported) and agree to 0.02-0.08%/amu, 0.02-0.11%/ amu and 0.04-0.11%/amu for $^{206}Pb/^{204}Pb$, $^{207}Pb/^{204}Pb$, and $^{208}Pb/^{204}Pb$, respectively. Maximum blank values for Sr, Nd, and Pb are 0.8, 0.2, and 0.7 ng, respectively. Helium was measured on the sample indicated except where sufficient glass was unavailable, in which case a chemically similar sample from the same dredge was used (D10-4, D14-8, D33-1, D51-3, D53-1). All helium values were measured by in vacuum crushing and have been blank corrected: a subset of ten samples was also measured for helium concentration by melting. Blanks were run before and after each sample, and samples were run only when blank variabilities were below 10%. Uncertainties in $^{3}He/^{4}He$ represent the 2σ quadrature sum of the in-run ion counting uncertainties on the ^{3}He beam, plus uncertainties due to blank variability and reproducibility of air standards, and are always <±0.06. Helium concentrations were determined by peak height comparison to calibrated volumes of air standards. Analaytical uncertainty in ^{4}He peak height is <1%. Duplicate helium isotope measurements of D61-1 are 8.40 R_A and 8.42 R_A and of D20-1 are 7.98 R_A and 7.96 R_A; averages are reported. Trace element (ppm) analyses were performed by inductively coupled plasma mass spectrometry (ICP-MS) at Cornell University in the laboratory of W. White and at Lamont-Doherty Earth Observatory, following sample preparation at Duke University; reproducibility for ICP-MS analyses, as judged by replicate dissolutions, is ±1-3% for Nd and Sm and ±1-6% for other elements. Complete major and trace element data for representative samples from each ridge segment are available from *Klein and Karsten* [1995] and *Sherman et al.* [1997].

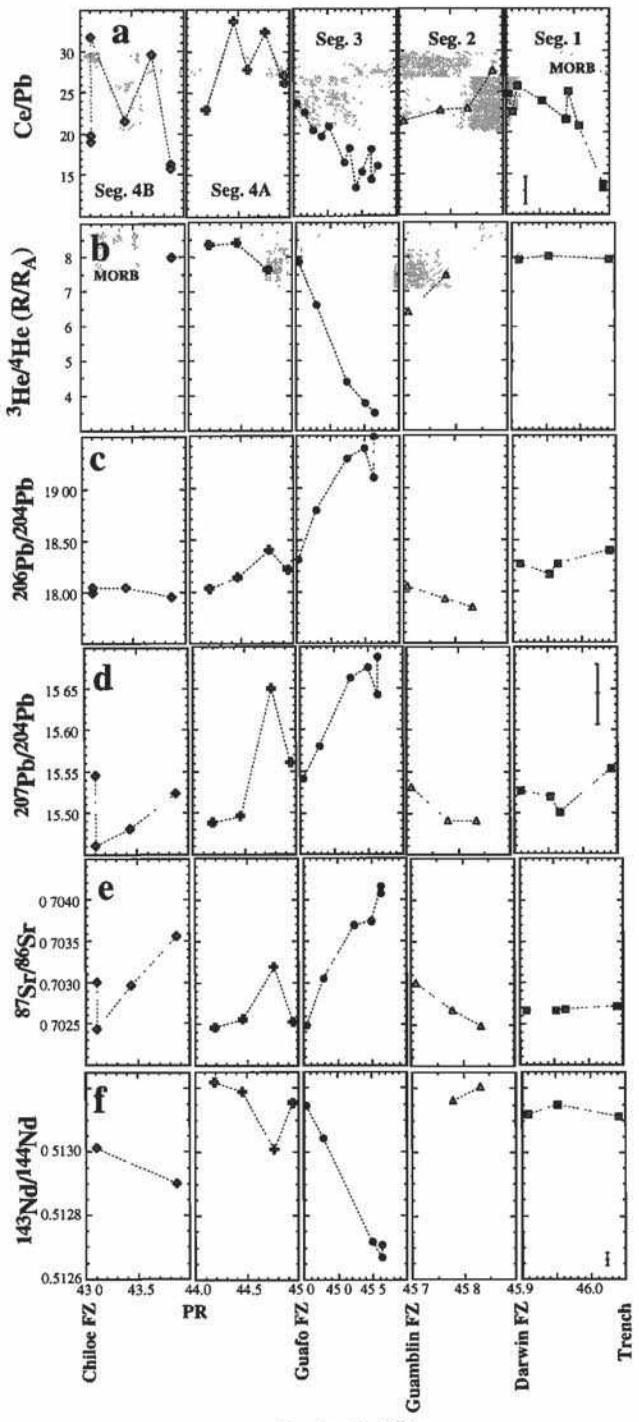

Figure 3. Latitude versus (a) Ce/Pb, (b) ^{3}He/^{4}He (R/ R$_A$), (c) ^{206}Pb/^{204}Pb, (d) ^{207}Pb/^{204}Pb, (e) ^{87}Sr/^{86}Sr, and (f) ^{143}Nd/^{144}Nd for Chile Ridge glasses (symbols as in Figure 1). Locations of the trench, fracture zones, and propagating rifts (PR) relative to the ridge segments are noted. Fields shown are for MORB [*Hofmann et al.*, 1986; *Hofmann*, 1988; *Sun and McDonough*, 1989; *Lupton and Craig*, 1975]. Analytical uncertainties (±2σ) that exceed symbol size are shown at right.

ment 2 lavas lie in the region of overlap between Atlantic-Pacific MORB and Indian Ocean MORB, although they extend to lower ^{206}Pb/^{204}Pb (to 17.8) and slightly elevated ^{87}Sr/^{87}Sr, ^{208}Pb/^{204}Pb, and ^{207}Pb/^{204}Pb compared to segments 1 and 3 and thus extend into the Indian Ocean MORB field (Figure 4).

4.4. Segment 4

Segment 4 lavas as a whole have affinities with the low ^{206}Pb/^{204}Pb and elevated ^{207}Pb/^{204}Pb and ^{208}Pb/^{204}Pb for a given ^{206}Pb/^{204}Pb often found in Indian Ocean MORB and OIB of the Dupal anomaly [e.g., *Mahoney et al.*, 1992; *Hart*, 1984], and they trend toward compositions associated with EM1-type localities (e.g., Gough Island and Walvis Ridge; Figure 4). On the basis of Pb-Sr-Nd isotopes, as well as major elements [*Sherman et al.*, 1997], segment 4 forms two geochemical provinces: a southern (4A) and northern (4B) group, bounded by a southward propagating rift (Figures 1 and 3) [*Tebbens et al.*, 1997]. Segment 4A lavas extend from a depleted end-member toward moderate ^{206}Pb/^{204}Pb (to 18.4) and very high ^{207}Pb/^{204}Pb (to 15.65; Figure 4) and show isotopic affinities with lavas from Gough Island (Figure 4) [*Sun*, 1980]. In contrast, segment 4B lavas extend from a depleted end-member like that of segment 4A but toward low ^{206}Pb/^{204}Pb (to 17.95) and elevated ^{207}Pb/^{204}Pb (to 15.54; Figure 4) and have isotopic affinities with lavas from Walvis Ridge [*Richardson et al.*, 1982]. Both segments 4A and 4B have typical MORB ^{3}He/^{4}He, and no clear along-axis systematics are apparent for either group (Figure 3).

The presence of MORB with Dupal anomaly characteristics [*Hart*, 1984] along segment 4 (43°S-45°S) offers some support for the controversial idea that the Dupal anomaly is indeed globe encircling in extent [*Castillo*, 1988]. While lavas with Dupal characteristics occur sporadically outside of 30-60°S [*Shirey et al.*, 1987; *Graham et al.*, 1988; *Roden et al.*, 1994], previous work has shown it to be most prevalent in this latitudinal band. In our sample suite the Dupal characteristics occur only in samples from segment 4, and previous sampling of the northern Chile Ridge at ~37°S shows no evidence of this anomaly [*Bach et al.*, 1996]. Therefore, although segment 4 provides evidence for the occurrence of the Dupal anomaly in the subridge mantle of the eastern Pacific, sampling to date suggests that the anomaly is not widespread.

5. Discussion

Each of the four transform-bounded segments along the southern Chile Ridge is compositionally unique. These spatial systematics suggest that the mantle in this region is heterogeneous with respect to He, Pb, Sr, and Nd isotopic composition and, by inference, to time-integrated U/He, U/Pb, Th/Pb, Rb/Sr, and Sm/Nd ratios, on a scale at least as small as that of the ridge segments (~50-100 km; Figure 1). Furthermore, within each ridge segment, there exists a range of compositions which demonstrate an even finer scale of source heterogeneity.

5.1. Segment 1

Klein and Karsten [1995] showed that segment 1 lavas display trace element signatures which suggest incorporation in their source of recycled, continentally derived material. The heavily sedimented nature of this ridge segment due to its location immediately adjacent to the trench raises the possibility that the observed recycled trace element signature (e.g., low Ce/Pb, Nb/U; Figure 2) may result from incorporation of ocean floor sediment during magma residence or upon eruption. In order to evaluate the feasibility of contamination via assimilation we have measured the isotopic and trace element composition of a nearby surface sediment (D24-1) and used it as the assimilant in a simple assimilation-fractional crystal-

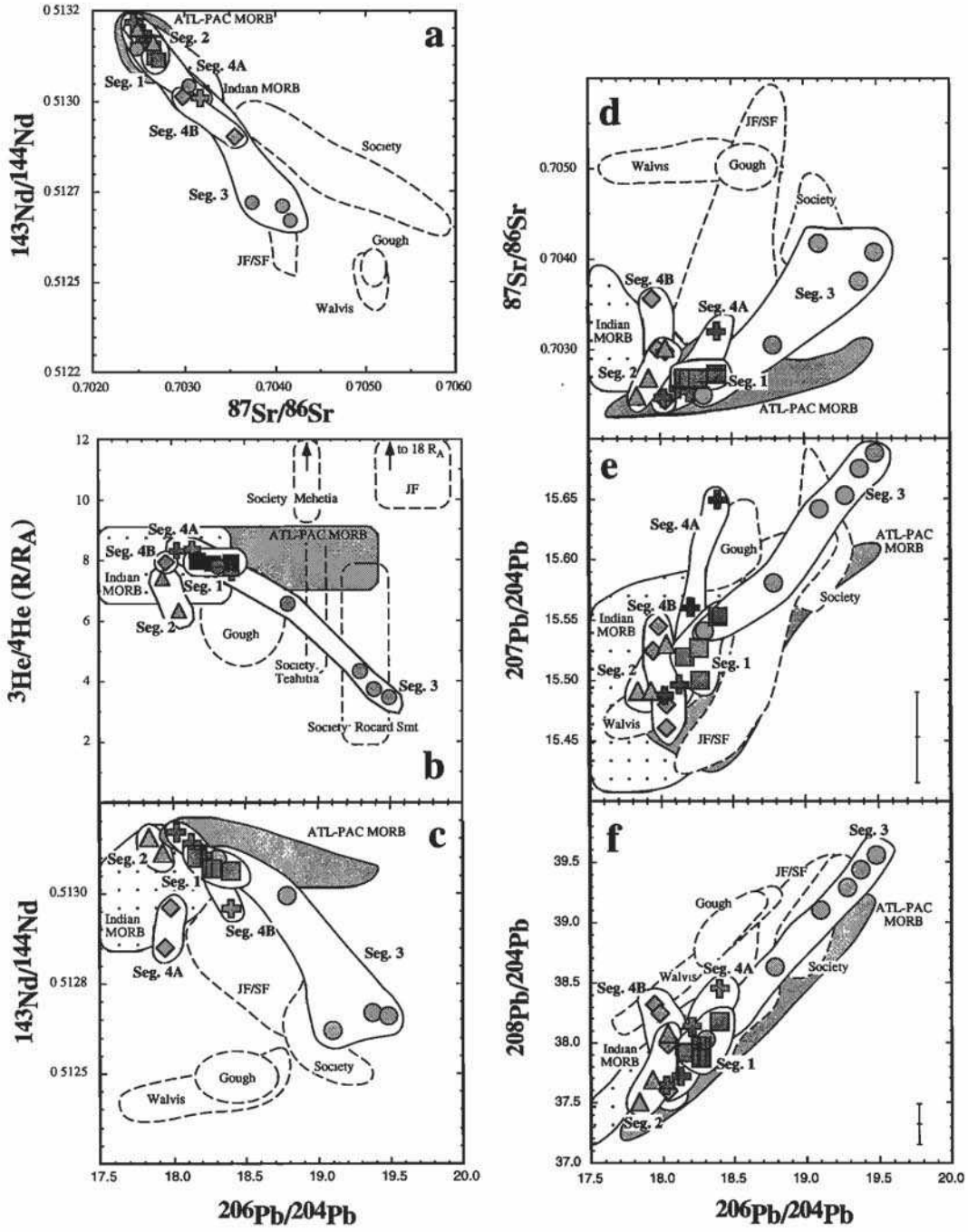

Figure 4. (a) $^{87}Sr/^{86}Sr$ versus $^{143}Nd/^{144}Nd$ and $^{206}Pb/^{204}Pb$ versus (b) $^{3}He/^{4}He$ (R/R_A) and (c) $^{143}Nd/^{144}Nd$, (d) $^{87}Sr/^{86}Sr$, (e) $^{207}Pb/^{204}Pb$ and (f) $^{208}Pb/^{204}Pb$ for Chile Ridge glasses (symbols as in Figure 1). Also shown are fields for Atlantic-Pacific MORB and Indian MORB, Gough Island, Walvis Ridge, Juan Fernandez Islands (JF), San Felix Islands (SF) and Society Islands (dashed lines). Data sources include *Sun* [1980], *Gerlach et al.* [1986], *Devey et al.* [1990], *Richardson et al.* [1982], *Hofmann et al.* [1986], *Hofmann* [1988], *Hart and Zindler* [1989], *Sun and McDonough* [1989], *Staudacher and Allègre* [1989], *Chauvel et al.* [1992], and *Farley et al.*, [1993]. Analytical uncertainties ($\pm 2\sigma$) that exceed symbol size are shown.

lization (AFC) model [*DePaolo*, 1981; *Reagan et al.*, 1987]. Results of the AFC calculations over a range of rates of assimilation to crystallization (R_a/R_c=0.01 to 0.9) fail to reproduce the segment 1 isotopic trends (e.g., Figure 5a) and in terms of trace elements form trends which, although they reproduce the segment 1 lavas on individual plots, require inconsistent parameters depending on the elements involved (e.g., Rb/Cs versus Cs suggests ~10% crystallization with R_a/R_c=0.01, while Nb/U versus Nb suggests ~70% crystallization with R_a/R_c =0.9; not shown). Similarly, assimilation (with fractional crystallization) of bulk marine sediment is also unable to reproduce the segment 1 trends (Figure 5a). These findings are in agreement with the conclusion of *Klein and Karsten* [1995], based solely on trace element arguments,

that contamination by bulk marine sediment does not reproduce the geochemical trends observed along segment 1.

While synvolcanic assimilation does not explain the geochemical trends observed along segment 1, the trace element signatures of segment 1 lavas strongly suggest contamination by recycled materials (Figures 2 and 5a and 5b). Following the modeling approach of *Klein and Karsten* [1995], we have explored a simple contamination model involving subduction of sediment (see Figure 5 caption) and altered oceanic crust, mixing of this recycled material with depleted mantle to form localized heterogeneities, and subsequent mixing of melts from the contaminated mantle with MORB melts. These model results reproduce both the trace element and isotopic trends observed along segment 1 (least well reproduced is the $^{87}Sr/^{87}Sr$ trend, which may require a higher MORB $^{87}Sr/^{87}Sr$ depleted end-member; Figure 5c). This suggests that only a small amount (~2%) of a recycled contaminant (consisting of ~20% sediment and ~80% altered crust) mixed into the depleted mantle is required to explain the segment 1 trace element and Pb, Sr, and Nd isotope trends.

Segment 1 lavas have relatively high $^{3}He/^{4}He$ values (~8 R_A). The timing of the recycling event for segment 1 can be roughly constrained through the $^{3}He/^{4}He$ systematics because this ratio can decrease over relatively short timescales due to the decay of U and Th. The high $^{3}He/^{4}He$ ratios of segment 1, therefore, can be used to estimate the amount of time which may have passed since recycling without producing a significant reduction in $^{3}He/^{4}He$. This calculation requires knowledge of the U/He ratio of the source which we estimate from the U and $[He]_{total}$ contents of the most enriched segment 1 sample

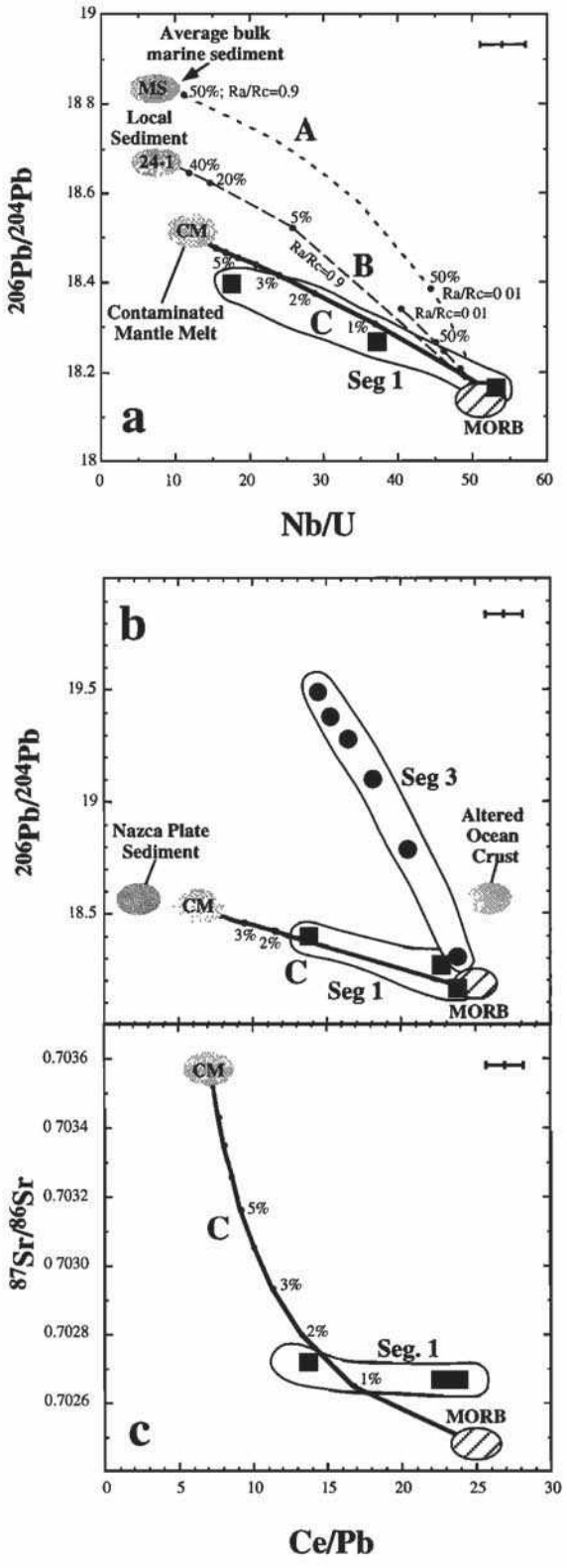

Figure 5. Evaluation of two contamination models for segment 1 glasses (squares). (a) Nb/U versus $^{206}Pb/^{204}Pb$; Ce/Pb versus (b) $^{206}Pb/^{204}Pb$ and (c) $^{87}Sr/^{86}Sr$. In Figure 5a, AFC trends using local sediment (D24-1; dashed lines) or bulk marine sediment (MS [*Ben Othman et al.*, 1989] dotted line) as assimilant with variable rates of assimilation to crystallization (R_a/R_c =0.01 and 0.9; labeled); percentages of crystallization are shown. Note that lines for R_a/R_c =0.01 and 0.9 overlap for MS case and 50% crystallization is shown for each R_a/R_c. Solid bold lines represent mixing (percent indicated) between a 10% MORB melt (oblique ruled oval) and a 10% melt derived from a mantle contaminated with 2% recently subducted contaminant (consisting of 20% sediment and 80% altered oceanic crust; oval labeled CM). For recycling model calculations, Nb, U, Ce, Pb, Sr, $^{87}Sr/^{86}Sr$, and $^{206}Pb/^{204}Pb$ in mantle source are 0.269, 0.005, 0.775, 0.031, 12, 0.70248, and 18.15, respectively [*Sun and McDonough*, 1989; *Stolper and Newman*, 1994; *Hart and Zindler*, 1989; *Hart and Staudigel*, 1989]; in subducted sediment they are 10, 1.6, 73, 20, 200, 0.71002, and 18.55, respectively [*Unruh and Tatsumoto*, 1976; *Ben Othman et al.*, 1989] (and local sediment D24-1); in altered crust they are 1.22, 0.275, 6.19, 0.23, 168, 0.70400 and 18.6, respectively [*Staudigel et al.*, 1995; *Chauvel et al.*, 1992; *Hart and Zindler*, 1989; *Dasch*, 1981]. Note that a marine sediment of intermediate composition compared to the global range [*Ben Othman et al.*, 1989; *Plank and Langmuir*, 1993; *Plank and Ludden*, 1992] and consistent with measurements of local sediments was used in these calculations because full trace element analyses are not available for the sediment section being subducted in this region [*Plank and Langmuir*, 1998]. Also shown in Figure 5b are fields for Nazca plate sediments and altered oceanic crust [*Unruh and Tatsumoto*, 1976; *Dasch*, 1981; *Sun and McDonough*, 1989; *Stolper and Newman*, 1994]. Bulk distribution coefficients for Nb, U, Ce, Pb and Sr for melting calculations and AFC models are 0.0085, 0.008, 0.011, 0.015, and 0.015, respectively [*Green*, 1994; *McCulloch and Gamble*, 1991; *Sun and McDonough*, 1989; *Stolper and Newman*, 1994]. Analytical uncertainties (±2σ) that exceed symbol size are shown.

(D20-1), adjusted for melting and degassing [after *Farley et al.*, 1992]. Sample D20-1 has a total [He] content (crushed plus melted) of 7.57 μcm^3 STP/g and a U content of 0.13 ppm (Table 1). If we assume that these measured abundances result from at least 10% partial melting [*Sherman et al.*, 1997] and from ~90% degassing during upwelling, residence, and eruption, the contaminated mantle source would have a U content of ~0.01 ppm and a U/He ratio of ~1700, a value consistent with the estimate of *Hart and Zindler* [1989]. Given this U/He ratio, a Th/U ratio of 3.8, and an assumed initial $^3He/^4He$ ratio of 8 R_A, a significant reduction of the $^3He/^4He$ ratio (to <7.94 R_A) would occur in ~20 Myr. A more conservative estimate of 50% degassing yields a reduction of the $^3He/^4He$ in only ~2 Myr. An extreme value of 99% degassing would produce a significant reduction in $^3He/^4He$ in ~200 Myr, but this would imply a mantle [He] near 75 $\mu cm^3/g$, even higher than the highest values found in mid-ocean ridge popping rocks [*Sarda and Graham*, 1990]. We infer that relatively short timescales (10^6 to 10^7 years) are involved for introduction of recycled components to the subridge mantle, suggesting that the unusual enriched signature in the segment 1 lavas may derive from contamination from the adjacent subduction zone.

The fact that the adjacent subduction zone is a plausible source of recycled material for segment 1 raises the important question about how these contaminants have been introduced into the subridge mantle. There are several possible mechanisms which may produce this result, and we can only speculate on which may occur here. First, as a young, hot, buoyant ridge approaches a trench, resistance to subduction may cause the subducting lithosphere to break up [*van den Buekel*, 1990], and as a result, portions of the slab (or slab-derived components) may founder or be sheared into the suboceanic mantle underlying segment 1 (Figure 6a). Second, continued spreading at the ridge following subduction may occur without magmatic accretion and may lead to the development of a "slab window" within a subduction zone [*Dickinson and Snyder*, 1979; *Thorkelson*, 1996; *Ramos and Kay*, 1992]. In this case, material derived from the subducting lithosphere or from the metasomatized mantle wedge may become entrained in lateral mantle flow feeding upwelling under the segment 1 ridge axis (Figure 6b), possibly carried by shallow, westward asthenospheric flow which has been postulated for this region [*Parmentier and Oliver*, 1979]. Third, the subducting spreading center may act to focus rising melt (which has been contaminated with slab components) back toward the trench, in a tunnel formed on the seaward side of the subducting lithosphere (Figure 6c). This latter mechanism may be most plausible because the most enriched samples along segment 1 lie closest to the trench. In any case, the mechanism must transport materials from the subarc mantle or the subducting lithosphere to the suboceanic mantle on timescales of tens of millions of years given the helium isotope arguments presented above.

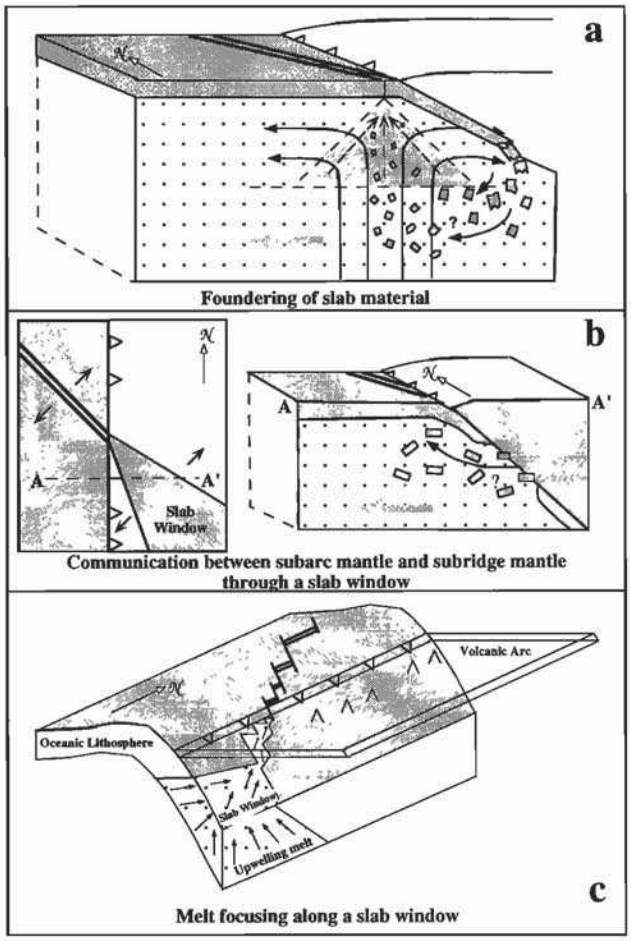

Figure 6. Schematic diagrams of a subducting spreading center that show possible modes of contamination of the segment 1 mantle. (a) Incorporation of slab-derived material into the melting regime beneath segment 1 as a result of foundering after slab breakup as postulated by *van den Buekel* [1990]. (b) A plan view (left) of development of a "slab window" [*Thorkelson*, 1996] and (right) a cross-sectional view which illustrate communication that may occur between metasomatized subarc mantle and the mantle beneath segment 1. Large gray arrows (in Figures 6a and 6b) represent shallow asthenospheric mantle flow postulated for this region [*Parmentier and Oliver*, 1979]. (c) A slab window occurs and focuses melt upward toward the trench as melt rises to fill the void formed by continued spreading. This melt incorporates recycled materials (perhaps in the form of contaminated fluids or melts) as it migrates upward along ridges and transform faults on the trenchward side of the slab and ultimately contaminates the segment 1 mantle source.

5.2. Segment 3

One of the most striking aspects of the chemical variations along segment 3 is the low helium isotope ratios (3.5 R_A compared to MORB of 7-9 R_A [*Kurz and Jenkins*, 1981; *Graham et al.*, 1992b]. Low $^3He/^4He$ ratios such as these, although not previously observed in MORB, have been found in some ocean islands and in island arc lavas and continental basalts [e.g., *Graham et al.*, 1988; *Hilton and Craig*, 1989; *Hilton et al.*, 1992; *Graham et al.*, 1993]. In the case of ocean islands, low ratios may result from pre-eruptive or post-eruptive degassing and subsequent ^4He ingrowth, rather than low $^3He/^4He$ in the mantle source [*Condomines et al.*, 1983; *Graham et al.*, 1988; *Hilton et al.*, 1995; *Zindler and Hart*, 1986; *Hart and Zindler*; 1989; *Staudacher and Allègre*, 1989]. For segment 3, however, the strong correlation of $^3He/^4He$ with all other radiogenic isotope ratios measured and with latitude, as well as the "zero age" of the lavas (rendering any post-eruptive ingrowth of ^4He insignificant), suggests that the low $^3He/^4He$ of segment 3, like the radiogenic Pb, Sr and

Nd isotope ratios, is an inherent characteristic of the enriched end-member in the segment 3 mantle source.

Klein and Karsten [1995] noted the low Ce/Pb, Nb/U, and Rb/Cs of segment 3 lavas and showed that like segment 1, incorporation of a small amount of subducted sediment and altered oceanic crust into the depleted MORB source can explain their unique trace element signatures (Figure 2). The isotope variations can be used to further examine the feasibility of this model and to place constraints on the age and origin of the contamination event. The isotopic characteristics of the enriched end-member in segment 3 lavas, particularly the high $^{207}Pb/^{204}Pb$, suggest that the contaminant is old: because of the relatively short half-life of ^{235}U, $^{207}Pb/^{204}Pb$ ratios were largely determined early in Earth's history [e.g., *Ben Othman et al.*, 1989; *White*, 1993]. Therefore high $^{207}Pb/^{204}Pb$ of the segment 3 enriched lavas must have been produced during a period of U/Pb enrichment early in Earth's history. The combined isotopes and the trace element systematics suggest two end-member scenarios, which differ in where radiogenic ingrowth occurred and when the contaminant was introduced into the mantle. At one extreme, the segment 3 signature may result from contamination by anciently subducted altered ocean crust (with high U/Pb) [*Chauvel et al.*, 1992] and sediment (with low Ce/Pb) [*Chauvel et al.*, 1992; *Ben Othman et al.*, 1989] followed by ingrowth during residence in the mantle. At the other extreme, the segment 3 signature may result from contamination by more recently recycled material derived from an old continental source [*White and Dupré*, 1986; *Ben Othman et al.*, 1989; *Devey et al.*, 1990; *Hanan and Graham*, 1996].

The latter hypothesis (recent recycling of old continental material) can be evaluated by examining the Pb isotopic compositions of nearby materials available for recycling. The isotopic compositions of sediments from Deep Sea Drilling Project (DSDP) Hole 319 on the Nazca plate [*Unruh and Tatsumoto*, 1976] and along segment 1 (D24-1; Table 1) do not have sufficiently radiogenic Pb isotope ratios to act as an appropriate contaminant for segment 3 lavas (Figure 7). Similarly, materials which may be eroding into the southern and central Chile Trench, including basement material from southern and central South America, and various lithologies including Andean volcanic rocks and terrigenous sediments also fail to provide a source with sufficiently radiogenic Pb isotopes (Figure 7) [*Kay et al.*, 1996, *Aitcheson et al.*, 1995; *Tilton and Barriero*, 1980; *Barreiro and Clark*, 1984; *Allègre et al.*, 1996; J. Tarney, personal communication, 1998]. This finding does not preclude incorporation of material from a more distant source and subduction zone which is recycling sediments containing a large proportion of old continental material [e.g., *White et al.*, 1985; *White and Dupré*, 1986] (Figure 7 inset) or, alternatively, from the southern South American lower crust (of unknown but presumably not "ancient" composition) by a process such as tectonic erosion of the basement by the subducting plate [e.g., *Cloos*, 1993]. Thus, while we cannot rule out a scenario involving recent recycling of old cratonic material, the lack of a nearby "smoking gun" of appropriate composition renders this less likely than the alternate scenario in which the segment 3 chemical variations are derived from an ancient recycling event (with ingrowth of radiogenic signatures occurring in the mantle). This latter explanation is also commonly invoked to explain the similar isotopic and trace element variations in ocean islands with recycled signatures (EMII) such as the Society Islands [e.g., *Chauvel et al.*, 1992; *Hémond et al.*, 1994; *White*, 1985; *White and Hofmann*, 1982] (Figure 4).

Modeling of the segment 3 variations in a manner similar to that developed for the Society Islands [e.g., *Chauvel et al.*, 1992; *Devey et al.*, 1990; *Staudacher and Allègre*, 1989] shows that the observed segment 3 trends can be reproduced by recycling a small amount of altered oceanic crust plus terrigenous sediment (e.g., ~8-15% contaminant consisting of ~3% terrigenous sediment and ~97% altered crust) to the mantle at ~2 Ga [e.g., *White and Hofmann* 1982; *Chauvel et al.*, 1992; *Weaver*, 1991a, 1991b; *Klein and Karsten*, 1995] (Figures 8 and 9). In contrast, mixtures of ancient pelagic sediment (in amounts >1%) with altered crust (Figure 8 and 9) and young mixtures of either pelagic or terrigenous sediment with altered oceanic crust (Figure 8) fail to reproduce the segment 3 trends. These models assume bulk addition of recycled components, rather than selective contamination as a result of processing within the subduction zone, because our understanding of how the composition of material returned to the mantle may differ from what is subducted is insufficient [cf. *Stolper and Newman*, 1994; *Plank and Langmuir*, 1998]. Recent work on volatiles on these samples, for example, suggests that a hydrous siliceous melt may be the phase in which recycled components were transferred to the segment 3 mantle source [*Sherman*, 1998].

The broadly defined age constraint for the segment 3 mantle contaminant (~2 ± 0.5 Ga) derives from the Pb isotopes (Figure 8a). Helium isotopes provide little constraint on the timing of ancient recycling events because the $^{3}He/^{4}He$ ratio changes rapidly over these timescales and because the U/He ratio of the mantle is poorly known [e.g., *Hart and Zindler*, 1989]. Nonetheless, model results using estimates of the mantle U/He ratio through time (Table 2) [*Hart and Zindler*, 1989] and using U/He values that vary over 3 orders of magnitude to bracket the uncertainty are broadly consistent with the ~2 (± 0.5) Ga timing of the segment 3 recycling event obtained through the Pb isotope modeling (Figure 8b).

In the context of our preferred model of ancient recycling for segment 3 the fact that the contaminant has retained its chemical integrity implies that the segment 3 contaminant experienced isolation from convective stirring in the mantle for most of its history. The regular along-axis variation and strongly binary nature of the trends formed by segment 3 lavas suggest that the contaminant is discrete and relatively homogeneous on a scale sampled by melting. The heterogeneity underlying the southernmost portion of segment 3 therefore appears to have a history which began more than a billion years ago, with subduction of a minor amount of terrigenous sediment and altered oceanic crust; thereafter, it remained isolated from mantle convection, perhaps stored as a raft of material in a boundary layer at depth [e.g., *McKenzie and O'Nions*, 1983; *McCulloch*, 1993; *Hanan and Graham*, 1996]. In the relatively recent past this small plum of material probably rose diapirically through the upper mantle and emerged beneath the southern portion of segment 3. Disturbance of the boundary layer in which this blob was originally stored may have been initiated by pulsation from the nearby subducted plate [*Larsen et al.*, 1996].

5.3. Segment 4

Segment 4 lavas differ from segment 1 and 3 lavas in both trace elements and isotopes (Figure 3). In particular, the iso-

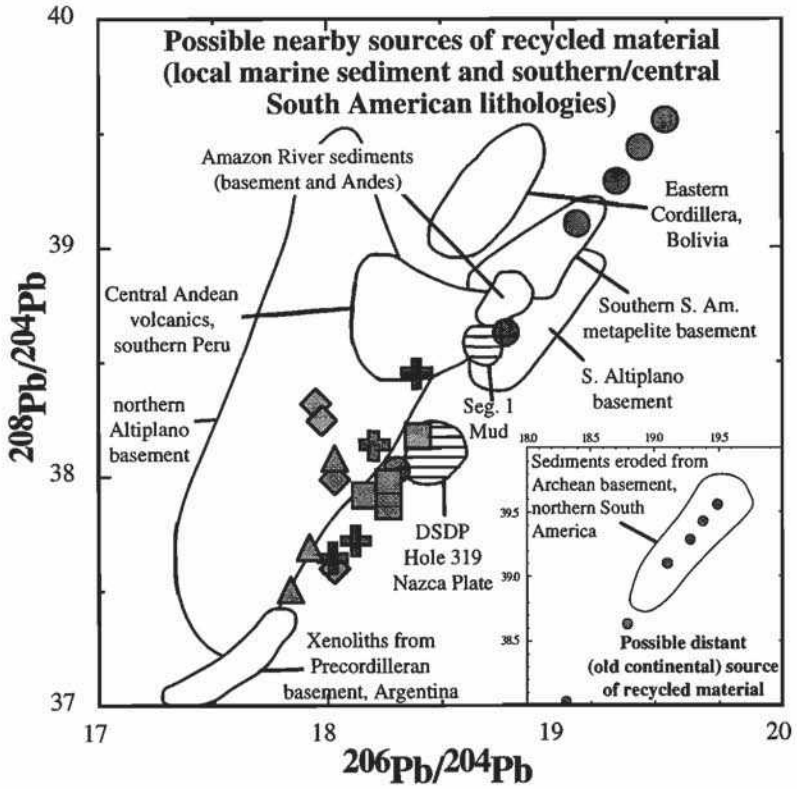

Figure 7. Evaluation of nearby and distant (inset) contaminants for segment 3 lavas (circles): $^{206}Pb/^{204}Pb$ versus $^{208}Pb/^{204}Pb$ for Chile Ridge glasses (symbols as in Figure 1). Also shown are fields for local sediment dredged from the segment 1 ridge axis (D24-1; horizontal ruled field) and Nazca plate sediment from DSDP Hole 319 (horizontal ruled field) [*Unruh and Tatsumoto*, 1976]. Fields for possible nearby sources of recycled material derived from southern and central South American lithologies include Amazon River sediments eroded from basement and Andes volcanics [*Allègre et al.*, 1996]; central Andean volcanics from southern Peru [*Barreiro and Clark*, 1984]; xenoliths from Precordilleran basement in Argentina [*Kay et al.*, 1996]; basement material (orthogneiss, schist) beneath the southern and northern Altiplano and the Eastern Cordillera centered in Bolivia [*Aitcheson et al.*, 1995; *Tilton and Barriero*, 1980]; and southern South American metapelitic basement material (samples provided by J. Tarney). Neither local sediment (horizontal ruled fields) nor any known South American lithologies (open fields) that may be currently subducted at the Chile Trench forms a suitable end-member for the segment 3 basalt array (solid circles). Inset shows possible distant source of recycled material derived from northern South American lithologies for segment 3 lavas; field shown for sediments sampled in front of the Antilles arc [*White et al.*, 1985] which eroded from Archean Guiana basement in northern South America [*White and Dupré*, 1986]. We cannot rule out possible incorporation of sediment from a distal old continental source that was subducted at a distant subduction zone and convectively conveyed to the mantle beneath segment 3.

topic variations reflect an affinity with Indian Ocean and Dupal compositions (Figure 4). The similarity to Indian Ocean MORB compositions raises the possibility that the unique geochemical signatures of segment 4 lavas may result from processes similar to those that produced the distinctive Indian Ocean MORB signature. Previous studies of Indian Ocean MORB have suggested that their particular isotopic characteristics may be due to an ancient, basin-wide, contamination event resulting from delamination of continental lithosphere possibly related to the breakup of Gondwanaland [e.g., *Mahoney et al.*, 1992; *Hart*, 1984]. Others, however, have called upon contamination via subduction of sediment with altered oceanic crust followed by homogenization in the mantle [e.g., *Hamelin et al.*, 1986; *Price et al.*, 1986; *le Roex et al.*, 1989; *Ito et al.*, 1987; *Michard et al.*, 1986; *Rehkämper and Hofmann*, 1997].

In a recent study of isotope and trace element data for Indian Ocean MORB, *Rehkämper and Hofmann* [1997] concluded that mixing a small amount of pelagic sediment and altered oceanic crust into an Atlantic-Pacific-type depleted mantle may explain the high $^{207}Pb/^{204}Pb$ b and $^{208}Pb/^{204}Pb$ observed in Indian Ocean MORB. They confirmed the findings of *Weaver* [1991b] that the low μ of pelagic sediment [*Ben Othman et al.*, 1989] results in substantially retarded ingrowth of $^{206}Pb/^{204}Pb$ relative to uncontaminated mantle with incorporation of only a few percent ancient pelagic sediment, a model which has also been invoked to explain EMI-type sources [e.g., *Weaver*, 1991b; *White and Hofmann*, 1982; *Chauvel et al.*, 1992]. Since the segment 4 lavas share some of the observed Indian Ocean (and EMI OIB) trace element (e.g., low Nb/U, high Ba/Nb) and isotopic characteristics, we examined a similar scenario for the development of the two

segment 4 signatures. These results suggest that the segment 4B systematics may be consistent with a simple contamination model consisting of three stages of isotope evolution and mixing of MORB melt with melts from mantle contaminated at least a billion years ago with pelagic sediment and altered oceanic crust (e.g., 10% contaminant consisting of 3-7% ancient pelagic sediment and 97-93% ancient altered crust; Figure 10 and Table 3). The higher $^{206}Pb/^{204}Pb$ (and lower $^{87}Sr/^{87}Sr$) of the segment 4A lavas can be explained by a somewhat greater proportion of altered oceanic crust in the recycled component compared to segment 4B lavas (Figure 10). Alternative scenarios such as recent recycling of sediment and altered oceanic crust [*Ben Othman et al.*, 1989], ancient recycling of pelagic sediment alone, or a two-stage Pb isotope evolution model (instead of a three-stage model [*White*, 1993]), fail to reproduce the segment 4 trends.

The trace element variations highlight another level of complexity in the history of the segment 4 source. Notably, the most isotopically enriched segment 4A samples have extremely high U/Pb (up to 0.44), while low U/Pb would be expected from the relatively low $^{206}Pb/^{204}Pb$ in the segment 4A lavas (Figure 10a inset and 10d). This factor of 5 variation in U/Pb (0.07 to 0.44) is unlikely to be due to variations in the extent of melting or crystal fractionation and suggests that a relatively recent enrichment event, perhaps metasomatic in origin, occurred in the mantle source but has not yet been manifest in the Pb isotopes. The high, but more homogenous U/Pb (0.20 to 0.23) of the segment 4B lavas coupled with their low $^{206}Pb/^{204}Pb$ (Figure 10a inset and 10d) suggests that the enrichment event also affected the segment 4B mantle source. Furthermore, the MORB-like $^{3}He/^{4}He$ ratios (7.97 to 8.41 R_A) of both segments 4A and 4B coupled with their high U abundances (up to 0.25 ppm; Table 1) suggest that this enrichment event occurred so recently that it has not yet affected the helium isotopes [e.g., *Hart and Zindler*, 1989]. Recent work on volatiles in these samples also suggest that the segment 4 mantle source has been metasomatized by an aqueous fluid [*Sherman*, 1998].

Although the helium isotope compositions are similar for both segment 1 and segment 4 (Figure 3), it is important to emphasize that the segment 4 inter-isotopic trends, as a whole, differ significantly from those of segment 1 (Figure 4). In the case of segment 1, all the isotopic and trace element evidence points toward a simple explanation of recent recycling of locally subducting sediment and altered oceanic crust.

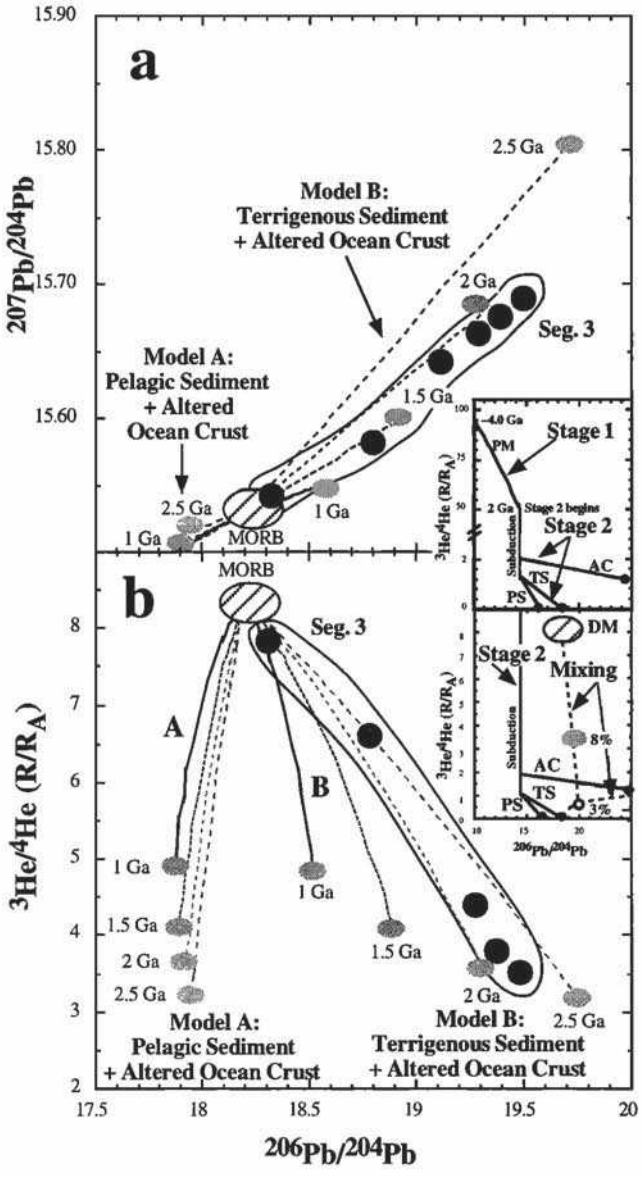

Figure 8. $^{206}Pb/^{204}Pb$ versus (a) $^{207}Pb/^{204}Pb$ and (b) $^{3}He/^{4}He$ (R/R_A) for segment 3 lavas (circles). Modeling results show that Pb isotopes (Figure 8a) require the timing of the recycling event for segment 3 to be ~2 (±0.5) Ga. $^{3}He/^{4}He$ (R/R_A) (Figure 8b), modeled using U/He values in Table 2 [*Hart and Zindler*, 1989], are also consistent with the ~2 Ga time since recycling (see text). Top inset shows two-stage model for ingrowth of $^{3}He/^{4}He$ and $^{206}Pb/^{204}Pb$ for primitive mantle (PM) from ~4.4 Ga to 2.0 Ga (stage 1) and for altered oceanic crust (AC), terrigenous sediment (TS) and pelagic sediment (PS) from 2.0 Ga to present; model parameters are given in Table 2. At the beginning of the second stage, altered oceanic crust with sediment is formed and subducted resulting in reduction of $^{3}He/^{4}He$. Note that the "two-stage" terminology is somewhat misleading because the crustal component reflects a multistage evolution that is not considered in this model. Solid circles show the present composition of aged pelagic and terrigenous sediment and altered oceanic crust. Bottom inset shows detail of top inset for mixing systematics (dashed lines) for producing contaminated mantle (model B) shown in Figure 8b. The contaminant (open circle labeled 3%) is a mixture of 3% terrigenous sediment and 97% altered oceanic crust. The contaminated mantle (shaded oval labeled 8%) is produced by mixing 8% of the terrigenous sediment-altered oceanic crust mixture with the depleted mantle (oblique ruled oval). Using these mixing proportions, different compositions of contaminated mantle result from variations in the time since the beginning of stage 2 and are shown in (Figures 8a and 8b) with aging of recycled material for 1, 1.5, 2, or 2.5 Ga (insets show ingrowth and mixing for 2 Ga example; thus the shaded oval in bottom inset is equivalent to the shaded oval labeled 2 Ga in (Figure 8b). The calculated trends (models A and B) in (Figures 8a and 8b) show mixing between a 10% melt derived from mantle contaminated 1-2.5 Ga (labeled shaded ovals) and a 10% MORB melt (oblique ruled oval). Bulk distribution coefficients for Pb and He for melting calculations are 0.015 and 0.008, respectively [*Stolper and Newman*, 1994; *Marty and Lussiez*, 1993].

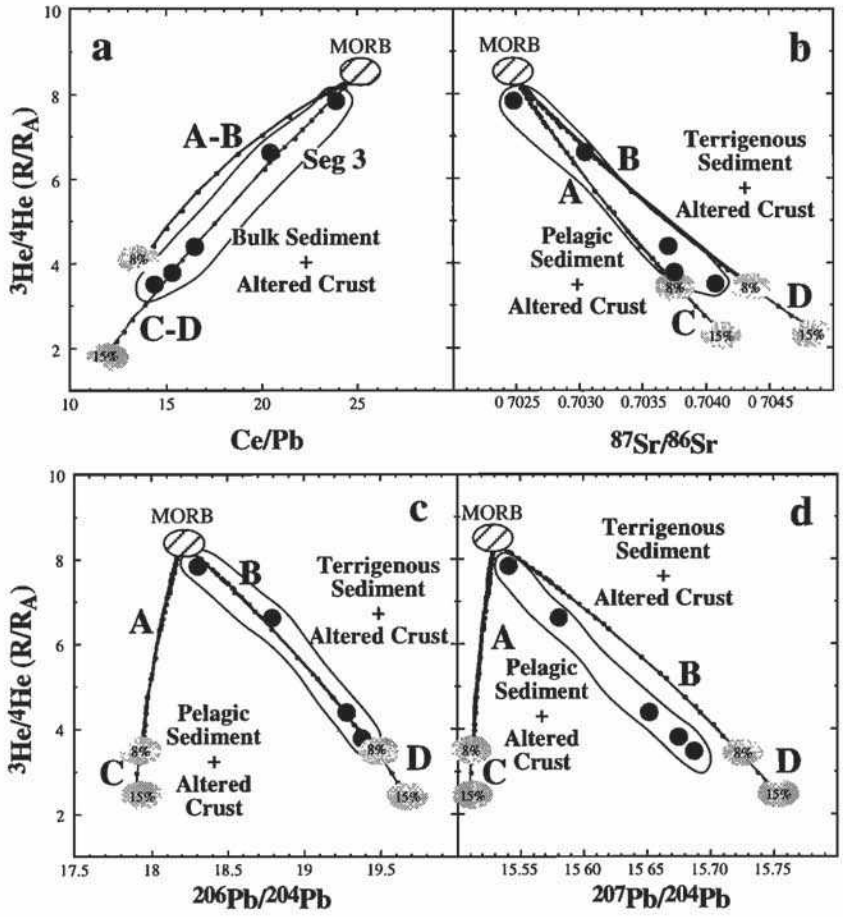

Figure 9. $^{3}He/^{4}He$ (R/R_A) versus (a) Ce/Pb, (b) $^{87}Sr/^{86}Sr$, (c) $^{206}Pb/^{204}Pb$, and (d) $^{207}Pb/^{204}Pb$ showing mixing systematics of the proposed contamination model for segment 3 glasses (solid circles; as discussed in the text and Figure 8 and Table 2). The calculated trends (models A, B, C, and D) show mixing between 10% melt derived from mantle variably contaminated with anciently recycled material (shaded ovals) and normal MORB melts (oblique ruled ovals) also produced by 10% melting. Models B and D show mixing between MORB melt and melt derived from mantle contaminated 2.2 Ga ago with 8 and 15% recycled altered ocean crust with terrigenous sediment in a 97-3% mixture; Models A and C are similar to models A and B except that pelagic instead of terrigenous sediment is incorporated. Ce/Pb and $^{3}He/^{4}He$ cannot resolve pelagic versus terrigenous sediment. Bulk distribution coefficients are from Figures 5 and 8 except for Nd, which is 0.005 [*Stolper and Newman*; 1994; *Green*, 1994]. Model parameters are reported in Table 2.

In the case of segment 4, however, the Pb isotopes require a poorly constrained but clear multistage evolutionary history. As a result, segment 4 lavas, like many of the Indian Ocean MORB they resemble, require a complex history involving several stages of variable enrichments over hundreds of millions to billions of years and at least one enrichment event that occurred relatively recently.

6. Conclusions

This study provides a window into the extensive degree of heterogeneity that is introduced into the depleted upper mantle by diverse processes associated with plate tectonic recycling. The largest variability along the southern Chile Ridge occurs on a scale of ~50-100 km, corresponding to the transform- and propagating-rift-bounded segmentation. A schematic drawing summarizing our conclusions is shown in Figure 11. The enriched signature of segment 1, strongest near the trench and diminishing to the north, shows evidence of recent contamination with terrigenous sediment and altered oceanic crust possibly related to the adjacent subduction zone. Segment 2 is the shortest ridge segment in the region and does not display a distinctive type of enrichment, although lavas erupted at its northern end appear to be influenced by material derived from a source similar to that at the southernmost end of segment 3 (located 50 km west). The radiogenic He, Pb, and Sr (and unradiogenic Nd) signature in segment 3 lavas, most pronounced in the south and diminishing gradually to the north, suggests a history of ancient subduction of altered oceanic crust plus terrigenous sediment which may have been recycled to the deep mantle and isolated from convective mixing for most of its history. The two geochemical groups of segment 4 (4A and 4B), separated spatially by a southward propagating rift, share the isotopic signature commonly associated with Indian Ocean MORB and Dupal compositions and show evidence of a complex history involving ancient recycling and a more recent enrichment event which decoupled trace element and isotope ratios.

Table 2. Segment 3 Model Parameters

	Primitive Mantle 4.55 Ga	NMORB Aged Since 4.55 Ga at 2.2 Ga	Continental Crust Pelagic Sediment Aged Since 4.55 Ga at 2.2 Ga	Continental Crust Terrigenous Sediment Aged Since 4.55 Ga at 2.2 Ga	Altered NMORB Aged Since 2.2 Ga at Present	Pelagic Sediment Aged Since 2.2 Ga at Present	Terrigenous Sediment Aged Since 2.2 Ga at Present	Depleted Mantle at Present
Rb	0.4				3.0	90	130	0.09
Th	0.09				0.07	9.5	14.3	0.019
U	0.024				0.24	1.6	3.1	0.005
Nb	0.713				1.22	10	10	0.223
Ce	1.775				6.19	73	73	0.78
Pb	0.185				0.23	22	20	0.03
Nd	1.3				11.2	38	30	0.83
Sr	21				168	290	190	10
Sm	0.444				3.75	6	6	0.38
[He] cm^3 STP/g					7.4E-05	1.0E-03	1.7E-03	6.5E-06
$^{87}Rb/^{86}Sr$	0.054	0.054	0.19	0.30	0.054	0.9	2	
$^{147}Sm/^{144}Nd$	0.21	0.19	0.14	0.17	0.19	0.09	0.12	
μ	8.2	8.2	8.2	8.2	26	4.6	10	
K	3.8	3.8	3.8	3.8	3.4	6.3	5	
U/He*		18,000			3250	1400	1790	
Ce/Pb	10	25	5	5	27	3	4	25
$^{3}He/^{4}He$ (R/R_A)*	103	50	0.03-90	0.03	2.1	0.03	0.03	8.4
$^{87}Sr/^{86}Sr$	0.69897	0.70151	0.70528	0.70915	0.70323	0.73384	0.77262	0.70248
$^{143}Nd/^{144}Nd$	0.50684	0.51009	0.50901	0.50947	0.51285	0.51031	0.51121	0.51315
$^{206}Pb/^{204}Pb$	9.307	14.38	14.38	14.38	24.96	16.25	18.45	18.20
$^{207}Pb/^{204}Pb$	10.294	15.03	15.03	15.03	16.49	15.29	15.59	15.53
$^{208}Pb/^{204}Pb$	29.487	34.00	34.00	34.00	44.16	37.33	39.75	38.00

Geochemical parameters are given that are used to model contamination of the mantle beneath segment 3. The isotopic compositions of altered MORB, pelagic sediment, and terrigenous sediment at 2.2 Ga were calculated using a single-stage evolution model, starting at 4.55 Ga with Basaltic Achondrite Best Initial [*Papanastassiou and Wasserburg*, 1969] for Sr isotopes; Moama achondrite [*Hamet et al.*, 1978] for Nd isotopes; Canyon Diablo [*Tatsumoto et al.*, 1973] for Pb isotopes; and *Hart and Zindler's* [1989] model for He isotope evolution of the mantle. U/He ratios noted for each stage are estimates from *Hart and Zindler's* [1989] model for helium isotope evolution of the Earth. $^{3}He/^{4}He$ of pelagic sediment at time of subduction varies depending on proportion of meteorical helium [e.g., *Ozima et al.*, 1984], but similar model results are obtained over a large range of values (0.03-90 R_A). Aged pelagic and terrigenous sediment at present has minimum possible $^{3}He/^{4}He$ considering the nucleogenic production of ^{3}He coupled to ^{4}He radiogenic production. Elemental abundances and parent/daughter ratios in altered oceanic crust and sediment are drawn from *Staudigel et al.* [1995], *Klein and Karsten* [1995], *Hart and Zindler* [1989]; *Staudacher and Allègre* [1989]; *Ben Othman et al.* [1989], *Plank and Langmuir* [1993]; *Plank and Ludden* [1992]; *Plank* [1993], and *Chauvel et al.* [1992]; depleted mantle source composition is from *Sun and McDonough* [1989], *Hofmann* [1988], *Stolper and Newman* [1994], *Rehkämper and Hofmann* [1997], *Hart and Zindler* [1989], and *Chauvel et al.*, [1992]. The parent/daughter ratios of the isotopic systems are in agreement with the listed trace element and isotopic data except for altered MORB (at present) whose μ and K were derived using the present-day isotope systematics of high μ (HIMU) basalts [*Rehkämper and Hofmann*, 1997]. Read 7.4E-05 as $7.4X10^{-5}$.

*These values are poorly constrained (see text).

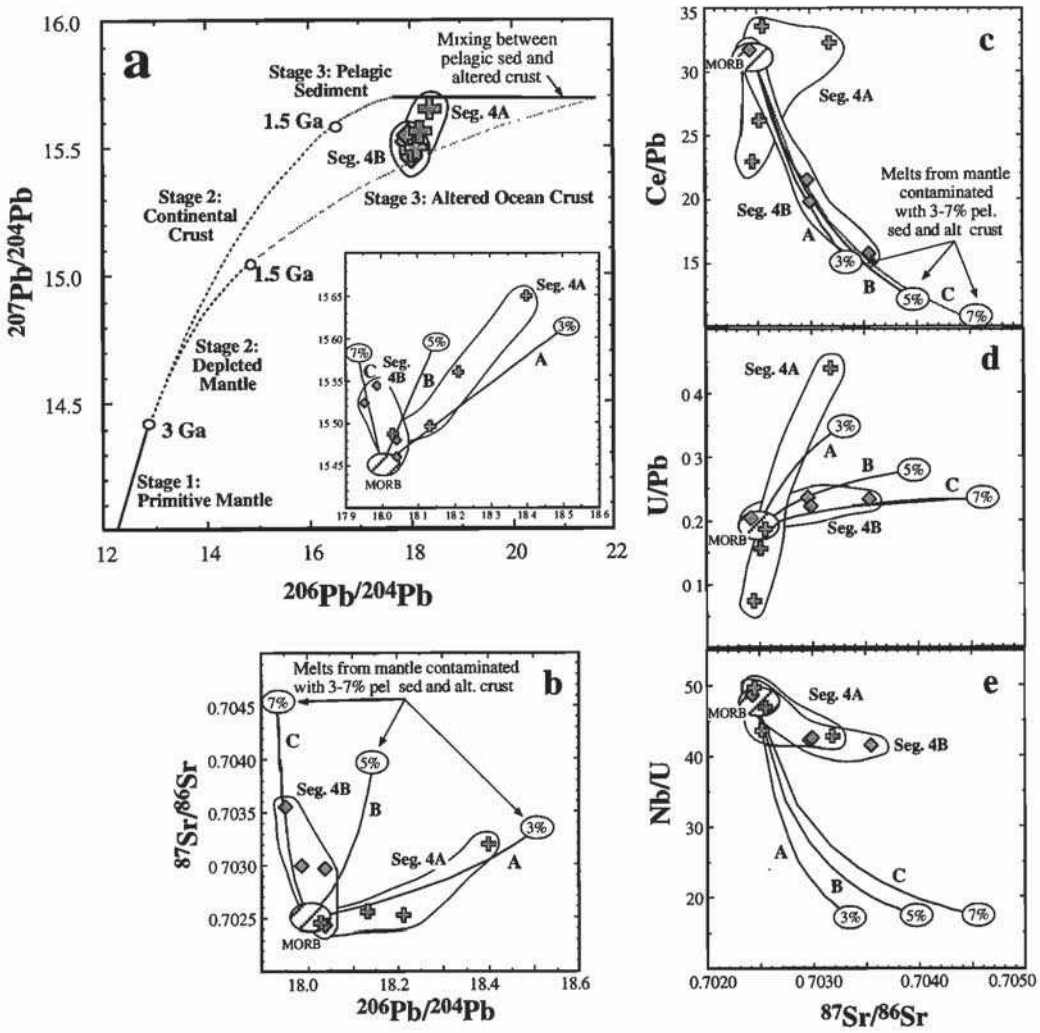

Figure 10. $^{206}Pb/^{204}Pb$ versus (a) $^{207}Pb/^{204}Pb$ and (b) $^{87}Sr/^{86}Sr$ and $^{87}Sr/^{86}Sr$ versus (c) Ce/Pb, (d) U/Pb, and (e) Nb/U showing mixing systematics for lavas from segment 4A (crosses) and 4B (diamonds). In Figure 10a, growth curves are shown for a three-stage isotopic evolution model for segment 4. The first stage (4.55-3.0 Ga; solid line) represents evolution of primitive mantle. The beginning of the second stage (at 3.0 Ga) marks the formation of the continental crust and depleted mantle (dashed lines are stage 2 growth curves for each). At the beginning of the third stage (1.5 Ga), oceanic crust is formed from the depleted mantle and hydrothermally altered, and pelagic sediment is deposited with a continental isotopic signature (dotted lines are stage 3 growth curves for each). Altered oceanic crust is subducted with pelagic sediment although their evolution is considered separately in the model. (Note that the "three-stage" terminology is somewhat misleading because the crustal component reflects a multistage evolution that is not considered here.) Recently, the altered crust and pelagic sediment mixed with depleted subridge mantle to form localized heterogeneities. During upwelling, these heterogeneities melt and the contaminated melts mix with depleted MORB melt (shown in Figure 10a inset). The calculated trends in the inset to Figure 10a and Figures 10b-10e show mixing between a 10% MORB melt (oblique ruled oval) and a 10% melt derived from mantle contaminated with 10% recycled material (consisting of 3% (model A), 5% (model B) and 7% (Model C) pelagic sediment with 97%, 95%, and 93% altered oceanic crust, respectively). Bulk distribution coefficients for melting calculations are from Figures 5 and 9. Elemental abundances and isotopic composition for model components during each stage are summarized in Table 3.

The approach taken in this study is based on the combined use of radiogenic isotopes and trace elements to identify plausible types and amounts of contaminants introduced into the mantle and their evolutionary history. While this is a common approach to model recycled signatures in MORB and OIB sources, it is underconstrained. Assumptions must be made about the bulk composition of altered oceanic crust based on limited exposures of the upper igneous section of modern seafloor and about the bulk composition of pelagic and terrigenous sediment, both of which are known to vary spatially and temporally. Futhermore, a consensus has not yet emerged on how the composition of material returned to the mantle differs from what is subducted. We are also only in the early stages of exploring the potential effects of recycling on the major element composition and mineralogy of the mantle and their resultant effects on melting parameters. Despite these uncer-

Table 3. Segment 4 Model Parameters

	Primitive Mantle at 4.55 Ga	Depleted Mantle Aged Since 4.55 Ga at 3.0 Ga	Continental Crust Aged Since 4.55 Ga at 3.0 Ga	Altered NMORB Aged Since 3 Ga at 1.5 Ga	Pelagic Sediment Aged Since 3 Ga at 1.5 Ga	Altered NMORB Aged Since 1.5 Ga at Present	Pelagic Sediment Aged Since 1.5 Ga at Present	Depleted Mantle at Present
Rb	0.635					3.0	90	0.09
Th	0.09					0.07	9.5	0.019
U	0.02					0.275	1.6	0.005
Nb	0.713					3.51	24	0.249
Ce	1.775					6.19	73	0.90
Pb	0.17					0.23	20	0.03
Nd	1.4					6.7	20	0.65
Sr	21					168	300	12
Sm	0.444					3.75	6	0.38
$^{87}Rb/^{86}Sr$	0.09	0.09	0.09	0.025	0.11	0.054	0.9	
$^{147}Sm/^{144}Nd$	0.19	0.19	0.19	0.21	0.6	0.19	0.09	
μ	8.2	8.2	8.2	9	9.5	26	4.6	
K	4	4	4	3	5	3.4	6.3	
Ce/Pb	10			27	3	27	4	25
Nb/U	32			15	15	13	15	47
$^{87}Sr/^{86}Sr$	0.69897	0.70097	0.70097	0.70151	0.71389	0.70226	0.72681	0.70248
$^{143}Nd/^{144}Nd$	0.50684	0.50878	0.50878	0.51085	0.50986	0.51272	0.51075	0.51315
$^{206}Pb/^{204}Pb$	9.307	12.86	12.86	15.83	16.00	22.64	17.20	18.20
$^{207}Pb/^{204}Pb$	10.294	14.41	14.41	15.37	15.43	16.01	15.54	15.53
$^{208}Pb/^{204}Pb$	29.487	32.52	32.52	33.27	36.46	40.08	38.69	38.00

Geochemical parameters are given that are used to model contamination of the mantle beneath segment 4. Calculations are similar to those in Table 2 except three stages of evolution were considered instead of two. Growth curves for all three stages are shown in Figure 10a. The trace element and isotopic composition of primitive mantle, continental crust, altered oceanic crust, pelagic sediment, and depleted mantle are drawn from references in Table 2.

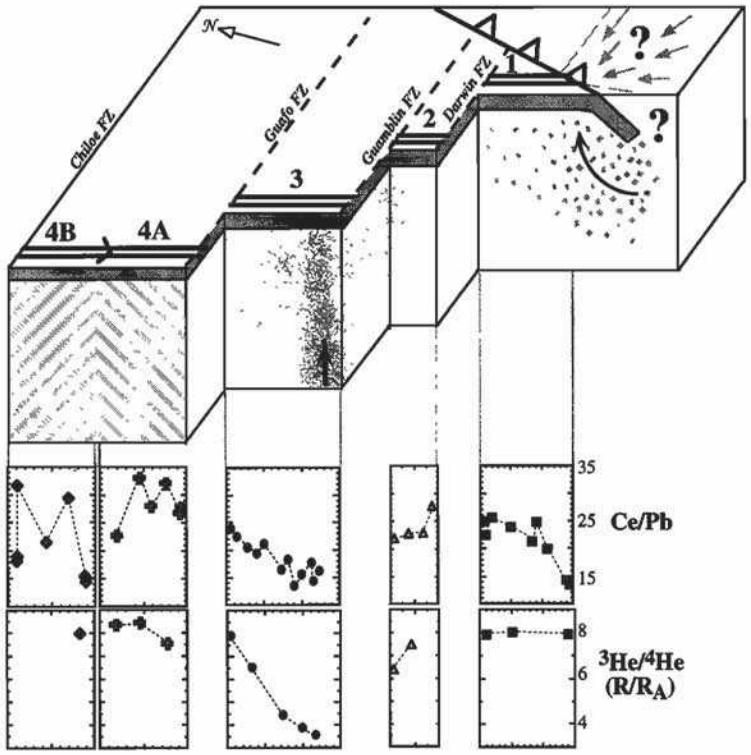

Figure 11. Schematic drawing illustrating the variability in the mantle source composition and histories for segments 1, 2, 3, 4A, and 4B as discussed in the text. Ridges (double lines), trench (barbed oblique line), fracture zones (FZ; dashed lines), and propagating rift along segment 4 (V) are indicated. A cross-sectional view of oceanic lithosphere is shown as shaded area for each segment and is subducting at the trench. Also shown are Ce/Pb and $^3He/^4He$ for each segment (symbols as in Figure 1). Mantle source composition for each segment is as required by the chemistry. Mantle beneath segment 1 may have been recently contaminated by recycled materials (small shaded blocks) or by contaminated melts (light shaded arrows) rising along the slab window (lightly shaded dashed lines; see Figure 6c). The discrete mantle heterogeneity beneath segment 3 is most readily explained by ancient recycling of continental material to the deep mantle, with more recent upwelling through the upper mantle. Mantle components beneath segments 4A and 4B differ from one another in detail, but share a common history of multistage evolution and possibly a more recent metasomatic enrichment.

tainties, the fact remains that trace elements and isotopes currently provide our best way to track the evolution of distinct portions of the mantle. Our results for the southern Chile Ridge show that unique combinations of isotope and trace element signatures can be used to constrain distinct evolutionary histories resulting from diverse recycling processes.

Acknowledgments. This paper has benefited from many thoughtful discussions with T. Plank, J. Karson, C. Langmuir, J. Douglass, S. L. Goldstein, P. Michael, C. Devey, J. Miller, S. B. Sherman, M. Stewart, and D. Curewitz. We especially thank Matthew Kohn, Bill White and an anonymous reviewer for their insightful and constructive comments. We also thank J. Lupton for providing access to the helium isotope laboratory which is supported by the NOAA Vents Program. This work was supported by grants from the National Science Foundation (OCE9116169, OCE9504280, and OCE9618736 to E. Klein, OCE9402506 to D. Graham, and OCE9116430 and OCE9503617 to J. Karsten).

References

Aitcheson, S. J., R. S. Harmon, S. Moorbath, A. Schneider, P. Soler, E. Soria-Escalante, G. Steele, I. Swainbank, and G. Worner, Pb isotopes define basement domains of the Altiplano, central Andes, *Geology, 23*, 555-558, 1995.

Allègre, C. J., and D. L., Turcotte, Geodynamic mixing in the mesosphere boundary layer and the origin of oceanic basalts, *Geophys. Res. Lett., 12*, 207-210, 1985.

Allègre, C. J., B. Hamelin, and B. Dupré, Statistical analysis of isotopic ratios in MORB: The mantle blob cluster model and the convective regime of the mantle, *Earth Planet. Sci. Lett., 71*, 71-84, 1984.

Allègre, C. J., B. Dupré, P. Negrel, and J. Gaillardet, Sr-Nd-Pb isotope systematics in Amazon and Congo River systems: Constraints about erosion processes, *Chem. Geol. 131*, 93-112, 1996.

Armstrong, R. L., A model for the evolution of strontium and lead isotopes in a dynamic earth, *Rev. Geophys., 6*, pp. 175-199, 1968.

Bach, W. J., Erzinger, L. Dosso, C. Bollinger, H. Bougault, J. Etoubleau, and J. Sauerwein, Unusually large Nb-Ta depletions in North Chile Ridge basalts at 36°50' to 38°56'S: Major element, trace element and isotopic data, *Earth Planet. Sci. Lett., 142*, 223-240, 1996.

Barreiro, B. A., and A. H. Clark, Lead isotopic evidence for evolutionary changes in magma-crust interaction, central Andes, southern Peru, *Earth Planet. Sci. Lett., 69*, 30-42, 1984.

Ben Othman, D., W. White, and J. Patchett, The geochemistry of marine sediments, island arc magma genesis, and crust-mantle recycling, *Earth Planet. Sci. Lett., 94*, 1-21, 1989.

Cande S. C., and R. B. Leslie, Late Cenozoic tectonics of the southern Chile trench, *J. Geophys. Res., 91*, 471-496, 1986.

Castillo, P., The Dupal anomaly as a trace of the upwelling lower mantle, *Nature, 336*, 667-670, 1988.

Chase, C. G., Ocean island Pb: Two-stage histories and mantle evolution, *Earth Planet. Sci. Lett., 52*, 277-284, 1981.

Chauvel, C., A. Hofmann, and P. Vidal, HIMU-EM: The French-Polynesian connection, *Earth Planet. Sci. Lett., 110*, 99-119, 1992.

Cloos, M., Lithospheric buoyancy and collisional orogenesis: Subduction of oceanic plateaus, continental margins, island arcs, spreading ridges, and seamounts, *Geol. Soc. Am. Bull., 105*; 715-737, 1993.

Condomines, M., K. Groenvald, P. J. Hooker, K. Muehlenbachs, R. K. O'Nions, N. Oskarsson, and E. R., Oxburgh, Helium, oxygen, strontium and neodymium isotopic relationships in Icelandic volcanics, *Earth Planet. Sci. Lett.*, *66*, 125-136, 1983.

Dasch, E. J., Lead isotopic composition of metalliferous sediments from the Nazca Plate, *Mem. Geol. Soc. Am.*, *154*, 199-209, 1981.

DePaolo, D. J., Trace element and isotopic effects of combined wall-rock assimilation and fractional crystallization, *Earth Planet. Sci. Lett.*, *53*, 189-202, 1981.

Devey, C. W., F. Albarede, J.-L. Cheminée, A. Michard, R. Mühe, and P. Stoffers, Active submarine volcanism on the Society hotspot swell (west Pacific): a geochemical study, *J. Geophys. Res.*, *95*, 5049-5066, 1990.

Dickinson, W. R., and W. S. Snyder, Geometry of subducted slabs related to San Andreas transform, *J. Geol.*, *87*, 609-627, 1979.

Dupuy, C., P. Vidal, H. G. Barsczus, and C. Chauvel., Origin of basalts from the Marquesas Archipelago (south central Pacific Ocean): Isotope and trace element constraints, *Earth Planet. Sci. Lett.*, *82*, 145-152, 1987.

Farley, K. A., J. H. Natland, and H. Craig, Binary mixing of enriched and undegassed (primitive?) mantle components (He, Sr, Nd, Pb) in Samoan lavas, *Earth Planet. Sci. Lett.*, *111*, 183-199, 1992.

Farley, K., A. R. Basu, and H. Craig, He, Sr, and Nd isotopic variations in lavas from the Juan Fernandez Archipelago, SE Pacific, *Contrib. Mineral. Petrol.*, *115*, 75-87, 1993.

Gerlach, D. C., S. R. Hart, W. J. Morales, and C. Palacios, Mantle heterogeneity beneath the Nazca plate: San Felix and Juan Fernandez islands, *Nature*, *322*, 165-169, 1986.

Graham, D. W., A. Zindler, M. D. Kurz, W. J. Jenkins, R. Batiza, and H. Staudigel, He, Pb, Sr, and Nd isotope constraints in magma genesis and mantle heterogeneity beneath young Pacific seamounts, *Contrib. Mineral. Petrol.*, *99*, 446-463, 1988.

Graham, D. W., J. Lupton, E. M. Klein, D. Christie, and D. Pyle, Helium isotope geochemistry of the Australian-Antarctic discordance, *Abstr. Geol. Soc. Aust.*, *27*; 41, 1990.

Graham, D. W., S. E. Humphris, W. J. Jenkins, and M. D. Kurz, Helium isotope geochemistry of some volcanic rocks from St. Helena, *Earth Planet. Sci. Lett.*, *110*, 121-131, 1992a.

Graham, D. W., W. J. Jenkins, J.-G. Schilling, G. Thompson, M. D. Kurz, and S. E. Humphris, Helium isotope geochemistry of mid-ocean ridge basalts from the South Atlantic, *Earth Planet. Sci. Lett.*, *110*, 133-147, 1992b.

Graham, D. W., P. Allard, C. R. J. Kilburn, F. J. Spera, and J. E. Lupton, Helium isotopes in some historical lavas from Mount Vesuvius, *J. Volcanol. Geotherm. Res.*, *58*, 359-366, 1993.

Green, T., Experimental studies of trace-element partitioning applicable to igneous petrogenesis-Sedona 16 years later, *Chem. Geol.*, *117*, 1-36, 1994.

Hamelin, B., B. Dupré, and C. J. Allègre, Pb-Sr-Nd isotopic data of Indian Ocean ridges: New evidence of large-scale mapping of mantle heterogeneities, *Earth Planet. Sci. Lett.*, *76*, 288-298, 1986.

Hamet, J., N. Nakamura, D. M. Unruh, and M. Tatsumoto, Origin and history of the eucrite, Moama as inferred from REE abundances, Sm-Nd and U-Pb systematics, *Proc. Lunar Planet. Sci. Conf.*, *1*, 1115-1136, 1978.

Hanan, B. B., and D. W. Graham, Lead and helium isotope evidence from oceanic basalts for a common deep source of mantle plumes, *Science*, *272*, 991-995, 1996.

Hart, S. and A. Zindler, Constraints on the nature and development of chemical heterogeneities in the mantle, in *Mantle Convection: Plate Tectonics and Global Dynamics*, edited by W. D. Peltier, pp. 261-387, Gordon and Breach, Newark, NJ, 1989.

Hart, S. R., A large-scale anomaly in the Southern Hemisphere mantle, *Nature*, *309*, 753-757, 1984.

Hart, S. R., A possible new Sr-Nd-Pb mantle array and consequences for mantle mixing, *Geochim. Cosmochim. Acta*, *50*, 1551-1557, 1986.

Hart, S. R., and C. Brooks, The geochemistry and evolution of the Early Precambrian mantle, *Contrib. Mineral. Petrol.*, *61*, 109-128, 1977.

Hart, S. R., and H. Staudigel, Isotopic characterization and identification of recycled components, in *Crust/Mantle Recycling at Convergence Zones*, edited by S. R. Hart and L. Gullen, pp. 15-28, Kluwer Acad. Pub., Norwell, Mass., 1989.

Hémond, C., C. W. Devey, and C. Chauvel, Source compositions and melting processes in the Society and Austral plumes (South Pacific Ocean): Element and isotope (Sr, Nd, Pb, Th) geochemistry, *Chem. Geol.*, *115*, 7-45, 1994.

Hickey, R., F. A. Frey, D. C. Gerlach, and L. Lopez-Escobar, Multiple sources for basaltic arc rocks from the southern volcanic zone of the Andes (34°-41°S): Trace element and isotopic evidence for contributions from subducted oceanic crust, mantle, and continental crust, *J. Geophys. Res.*, *91*, 5963-5983, 1986.

Hilton, D. R., and H. Craig, A helium isotope transect along the Indonesian archipelago, *Nature*, *342*, 906-908, 1989.

Hilton, D. R., J. A. Hoogewerff, M. J. van Bergen, and K. Hammerschmidt, Mapping magma sources in the east Sunda-Banda arcs, Indonesia: Constraints from helium isotopes, *Geochim. Cosmochim. Acta*, *56*, 851-859, 1992.

Hilton, D. R., J. Barling, and G. E. Wheller, Effect of shallow-level contamination on the helium isotope systematics of ocean-island lavas, *Nature*, *373*, 330-333, 1995.

Hofmann, A. W., Chemical differentiation of the Earth: The relationship between mantle, continental crust, and oceanic crust, *Earth Planet. Sci. Lett.*, *90*, 297-314, 1988.

Hofmann, A. W., and W. M White, The role of subducted oceanic crust in mantle evolution, *Carnegie Inst. Washington Publ.*, *79*, 477-483, 1980.

Hofmann, A. W., and W. M White, Mantle plumes from ancient oceanic crust, *Earth Planet. Sci. Lett.*, *57*, 421-436, 1982.

Hofmann, A. W., K. Jochun, M. Seufert, and W. M. White, Nb and Pb in basalts: New constraints on mantle evolution, *Earth Planet. Sci. Lett.*, *79*, 33-45, 1986.

Ito, E., W. M. White, and C. Göpel, The O, Sr, Nd and Pb isotope geochemistry of MORB, *Chem. Geol.*, *62*, 157-176, 1987.

Karsten, J. L., E. M. Klein, and S. B. Sherman, Subduction zone geochemical characteristics in ocean ridge basalts from the southern Chile Ridge: Implications of modern ridge subduction systems for the Archean, *Lithos*, *37*, 143-161, 1996.

Kay, S. M., S. Orrell, and J. M. Abbruzzi, Zircon and whole rock Nd-Pb isotopic evidence for a Grenville age and a Laurentian origin for the basement of the Precordillera in Argentina, *J. Geol.*, *104*, 637-648, 1996.

Klein,. E. M., and J. L. Karsten, Ocean-ridge basalts with convergent margin geochemical affinities from the Chile Ridge, *Nature*, *374*, 52-57, 1995.

Kurz, M. D., and W. J. Jenkins, The distribution of helium in oceanic basalt glasses, *Earth. Planet. Sci. Lett.*, *53*, 41-54, 1981.

Larsen, T. B., D. A. Yuen, J. L. Smedsmo, and A. V. Malevsky, Thermomechanical modeling of pulsation tectonics and consequences on lithospheric dynamics, *Geophys. Res. Lett.*, *23*, 217-220, 1996.

le Roex, A., H. J. B. Dick, and R. L. Fisher, Petrology and geochemistry of MORB from 25°E to 46°E along the Southwest Indian Ridge: Evidence for contrasting styles of mantle enrichment, *J. Petrol.*, *30*, 947-986, 1989.

Lupton, J. E., and H. Craig, Excess He-3 in oceanic basalts: Evidence for terrestrial primordial helium, *Earth. Planet. Sci. Lett.*, *26*, 133-139, 1975.

Mahoney, J., J. H. Natland,. W. H. White, R. Poreda, S. H. Bloomer, R. L. Fisher, and A. N. Baxter, Isotopic and geochemical provinces of the Indian Ocean spreading centers, *J. Geophys. Res.*, *94*, 4033-4052, 1989.

Mahoney, J., A. le Roex, Z. Peng, R. L. Fisher, J. H. Natland, Southwestern limits of the Indian Ocean Ridge mantle and the origin of low $^{206}Pb/^{204}Pb$ mid-ocean ridge basalt: Isotope systematics of the central Southwest Indian Ridge [17°-50°E], *J. Geophys. Res.*, *97*, 19771-19790, 1992.

Mahoney, J. J., J. M. Sinton, M. D. Kurz, J. D. MacDougall, K. J. Spencer, and G. W. Lugmair, Isotope and trace element characteristics of a super-fast spreading ridge: East Pacific Rise, 13-23°S, *Earth Planet. Sci. Lett.*, *121*, 173-193, 1994.

Manhes, G., J. F. Minster, and C. J. Allègre, Comparative uranium-thorium-lead and rubidium-strontium study of the Saint Severin amphoterite: Consequences for early solar system chronology, *Earth Planet. Sci. Lett.*, *39*, 14-24, 1978.

Marty, B., and P. Lussiez, Constraints on rare gas partition coefficients from a picritic mid-ocean ridge basalt, *Chem. Geol.*, *106*, 1-7, 1993.

McCulloch, M. T., The role of subducted slabs in an evolving Earth *Earth Planet. Sci. Lett.*, *115*, 89-100, 1993.

McCulloch, M. T., and J. A. Gamble, Geochemical and geodynamical constraints on subduction zone magmatism, *Earth Planet. Sci. Lett.*, *102*, 358-374, 1991.

McKenzie, D., and R. K. O'Nions, Mantle reservoirs and ocean island basalts, *Nature*, *301*, 229-231, 1983.

Michard, A., R. Montigny, and R. Schlich, Geochemistry of the mantle

beneath the Rodriguez Triple Junction and the Southeast Indian Ridge, *Earth Planet. Sci. Lett.*, *78*, 104-114, 1986.

Niu, Y., and R. Batiza, Trace element evidence from seamounts for recycled oceanic crust in the eastern Pacific mantle, *Earth Planet. Sci. Lett.*, *148*, 471-483, 1997.

Ozima, M., M. Takayanagi, S. Zashu, and S. Amari, High $^{3}He/^{4}He$ ratio in ocean sediments, *Nature*, *311*, 448-450, 1984.

Palacz, Z. A., and A. D. Saunders, Coupled trace element and isotope enrichment in the Cook-Austral-Samoa islands, southwest Pacific, *Earth Planet. Sci. Lett.*, *79*, 270-280, 1986.

Papanastassiou, D. A., and G. J. Wasserburg, Initial strontium isotopic abundances and the resolution of small time differences in the formation of planetary objects, *Earth Planet. Sci. Lett.*, *5*, 361-376, 1969.

Parmentier, E. M., and J. E. Oliver, A study of shallow global mantle flow due to the accretion and subduction of lithospheric plates. *Geophys. J. R. Astron. Soc.*, *57*, 1-21, 1979.

Plank, T., Mantle melting and crustal recycling in subduction zones, Ph.D. dissertation, Columbia Univ., New York, 1993.

Plank, T., and C. H. Langmuir, Tracing trace elements from sediment input to volcanic output at subduction zones, *Nature*, *362*, 739-742, 1993.

Plank, T., and C. H. Langmuir, The chemical composition of subducting sediment and its consequences for the crust and mantle, *Chem. Geol.*, *145*, 325-394, 1998.

Plank, T., and J. N. Ludden, Geochemistry of sediments in the Argo abyssal plain at Site 765: A continental margin reference section for sediment recycling in subduction zones, *Proc. Ocean Drill. Program Sci. Results*, *123*, 167-189, 1992.

Price, R. C., A. K. Kennedy,. M. Riggs-Sneeringer, and F. A. Frey, Geochemistry of basalts from the Indian Ocean Triple Junction: implications for the generation and evolution of Indian Ocean Ridge basalts, *Earth Planet. Sci. Lett.*, *78*, 379-396, 1986.

Ramos, A., and S. M. Kay, Southern Patagonia plateau basalts and deformation: Back-arc testimony of ridge collisions, *Tectonophysics*, *205*, 261-282, 1992.

Reagan, M. K., J. B. Gill, E. Malavassi, and M. O. Garcia, Changes in magma composition at Arenal volcano, Costa Rica, 1968-1985: Real-time monitoring of open-system differentiation, *Bull. Volcanol.*, *49*, 415-434, 1987.

Rehkämper, M., and A. W. Hofmann, Recycled ocean crust and sediment in Indian Ocean MORB, *Earth Planet. Sci. Lett.*, *147*, 93-106, 1997.

Richard, P., Shimizu, N. and Allègre, C. J., $^{143}Nd/^{146}Nd$, a natural tracer: An application to oceanic basalts, *Earth, Planet. Sci. Lett.*, *31*, 269-278, 1976.

Richardson, S. H., A. J. Erlank, A. R. Duncan, and D. L. Reid, Correlated Nd, Sr and Pb isotope variation in Walvis Ridge basalts and implications for the evolution of their mantle source, *Earth Planet. Sci. Lett.*, *59*, 327-342, 1982.

Ringwood, A. E., Phase transformations and differentiation in subducted lithosphere: Implications for mantle dynamics, basalt petrogenesis, and crustal evolution, *J. Geol.*, *90*, 611-643, 1982.

Roden, M. F., T. Trull, S. R. Hart, and F. A. Frey, New He, Nd, Pb, and Sr isotopic constraints on the constitution of the Hawaiian plume: Results from Koolau Volcano, Oahu, Hawaii, USA, *Geochim. Cosmochim. Acta*, *58*, 1431-1440, 1994.

Sarda, P. and D. Graham, Mid-ocean ridge popping rocks; implications for degassing at ridge crests, *Earth Planet. Sci. Lett.*, *97*, 268-289, 1990.

Schilling, J.-G., G. Thompson, R. Kingsley, and S. E. Humphris, Hotspot-migrating ridge interaction in the South Atlantic, *Nature*, *313*, 187-191, 1985.

Sherman, S. B., Influences of ridge subduction on mid-ocean ridge processes: Petrologic observations from the southern Chile Ridge and the Woodlark Basin, Ph.D. dissertation, University of Hawaii at Manoa, Honolulu, 1998.

Sherman, S. B., J. L. Karsten, and E. M. Klein, Petrogenesis of axial lavas from the southern Chile Ridge: Major element constraints, *J. Geophys. Res.*, *102*, 14,963-14,990, 1997.

Shirey, S. B., J. F. Bender, and C. H. Langmuir, Three-component isotopic heterogeneity near the Oceanographer Transform, Mid-Atlantic Ridge, *Nature*, *325*, 217-223, 1987.

Staudacher, T., and C. J. Allègre, Noble gases in glass samples from Tahiti: Teahitia, Rocard, and Mehetia, *Earth Planet. Sci. Lett.*, *93*, 210-222, 1989.

Staudigel, H., G. R. Davies, S. R. Hart, K. M. Marchant, and B. M. Smith, Large scale isotopic Sr, Nd and O isotopic anatomy of altered oceanic crust: DSDP/ODP sites 417/418, *Earth Planet. Sci. Lett.*, *130*, 169-185, 1995.

Stolper, E., and S. Newman, The role of water in the petrogenesis of Mariana trough magmas, *Earth Planet. Sci. Lett.*, *121*, 293-325, 1994.

Sun, S.-S., Pb isotopic study of young volcanic rocks from mid-ocean ridges, ocean islands and island arcs, *Philos. Trans. R. Soc. London, Ser. A*, *297*, 409-446, 1980.

Sun, S.-S., and W. F. McDonough, Chemical and isotopic systematics of oceanic basalts: Implications for mantle composition and processes, in *Magmatism in the Ocean Basins*, edited by A. D. Saunders and M. J. Norry, *Geol. Soc. Spec. Publ.*, *42*, 313-345, 1989.

Tatsumoto, M., R. J. Knight, and C. J. Allègre, Time differences in the formation of meteorites as determined from the ratio of lead-207 to lead-206, *Science*, *180*, 1279-1283, 1973.

Taylor, S. R. and McLennan, S. M., *The continental crust: Its composition and evolution*, 312 pp., Blackwell Scientific, Oxford, England, 1985.

Tebbens, S. F., S. Cande, L. Kovacs, J. C. Parra, J. L. LeBrecque, and H. Vergara, The Chile Ridge: A tectonic framework, *J. Geophys. Res.*, *102*, 12,035-12,059, 1997.

Thorkelson, D. J., Subduction of diverging plates and the principles of slab window formation, *Tectonophysics*, *255*, 47-63, 1996.

Tilton, G. R., and B. A. Barriero, Origin of lead in Andean calcalkaline lavas, southern Peru, *Science*, *210*, 1245-1247, 1980.

Unruh, D. M., and M. Tatsumoto, Lead isotopic composition and uranium, thorium, and lead concentrations in sediments and basalts from the Nazca plate, *Initial Rep. Deep Sea Drill. Proj.*, *34*, 341-347, 1976.

van den Beukel, J., Breakup of young oceanic lithosphere in the upper part of a subduction zone: Implications for the emplacement of ophiolites, *Tectonics*, *9*, 825-844, 1990.

Weaver, B. L., Trace element evidence for the origin of ocean-island basalts, *Geology*, *19*, 123-126, 1991a.

Weaver, B. L., The origin of ocean island basalt end-member compositions: Trace element and isotopic constraints, *Earth Planet. Sci. Lett.*, *104*, 381-397, 1991b.

White, W. M., Sources of oceanic basalts: Radiogenic isotopic evidence, *Geology*, *13*, 115-118, 1985.

White, W. M., $^{238}U/^{204}Pb$ in MORB and open system evolution of the depleted mantle, *Earth Planet. Sci. Lett.*, *115*, 211-226, 1993.

White, W. M., and B. Dupré, Sediment subduction and magma genesis in the lesser Antilles: Isotopic and trace element constraints, *J. Geophys. Res.*, *91*, 5927-5941, 1986.

White, W. M., and A. W. Hofmann, Sr and Nd isotope geochemistry of oceanic basalts and mantle evolution, *Nature*, *296*, 821-825, 1982.

White, W. M., B. Dupré, and P. Vidal, Isotope and trace element geochemistry of sediments from the Barbados Ridge-Demerara Plain region, Atlantic Ocean, *Geochim. Cosmochim. Acta*, *49*, 1875-1886, 1985.

Zindler, A., and S. Hart, Helium: Problematical primordial signals, *Earth Planet. Sci. Lett.*, *79*, 1-8, 1986.

Zindler, A., E. Jagoutz, and S. Goldstein, Nd, Sr and Pb isotopic systematics in a three-component mantle: A new perspective, *Nature*, *298*, 519-523, 1982.

E. M. Klein and M. E. Sturm, Division of Earth and Ocean Sciences, Nicholas School of the Environment, Duke University, Durham, NC 27708. (klein@geo.duke.edu; msturm@geo.duke.edu)

D. W. Graham, College of Oceanic and Atmospheric Sciences, Oregon State University, Corvallis, OR 97331. (dgraham@oce.orst.edu)

J. Karsten, School of Ocean and Earth Science and Technology, University of Hawaii at Manoa, Honolulu, HI 96822. (karsten@soest.hawaii.edu)

(Received April 10, 1998; revised October 28, 1998;
accepted December 3, 1998.)